

# 000 001 AUDITING TEST DATA CONTAMINATION WITH ERROR 002 RATE CONTROL FOR RELIABLE LLM EVALUATION 003 004

005 **Anonymous authors**

006 Paper under double-blind review

## 007 008 009 ABSTRACT

010 011 012 Large language models (LLMs) have achieved impressive performance across  
013 diverse tasks, largely driven by large-scale pretraining data. However, this data  
014 abundance has led to a critical issue: test data contamination, where benchmark  
015 datasets inadvertently overlap with pretraining corpora. This contamination com-  
016 promises the reliability of LLM evaluation by making it difficult to distinguish  
017 genuine generalization from memorization. To address this challenge, existing  
018 training data detectors aim to identify clean (unseen) data within potentially con-  
019 tampered test sets. While effective to some extent, these methods often misclassify  
020 contaminated data as clean due to the black-box nature of LLMs, resulting in  
021 residual contamination and unreliable evaluation. This raises a key question: Can  
022 we control the proportion of contaminated data mistakenly identified as clean i.e.,  
023 false discovery rate (FDR), below a user-specified threshold, while maximizing the  
024 amount of clean data retained for evaluation? Thus, we propose TD4Eval, a prin-  
025 cipled framework for training data detection that simultaneously ensures strict FDR  
026 control and high detection power. Specifically, we propose a rejection-count-based  
027 adaptive weighting strategy that learns the relative contribution of each detector.  
028 Based on these weights, we integrate multiple complementary detectors and ap-  
029 ply the Benjamini-Hochberg (BH) procedure to control the FDR. Theoretically,  
030 we show that TD4Eval achieves asymptotic optimality in controlling FDR and  
031 maintaining high power. Empirical results on real-world datasets demonstrate that  
032 TD4Eval achieves an average 30% improvement in FDR over SOTA methods.

## 033 1 INTRODUCTION

034 Large language models (LLMs) have demonstrated remarkable capabilities across a wide range of  
035 domains, largely due to the massive volumes of data used during pretraining Cheng et al. (2025);  
036 Chang et al. (2024). However, despite these impressive achievements, the uncontrolled expansion of  
037 data has introduced the problem of data contamination, where test datasets are inadvertently included  
038 in the training corpus. This contamination makes it difficult to determine whether a model has  
039 genuinely acquired a capability or is simply memorizing test data, thereby undermining the reliability  
040 of evaluation Zhang et al. (2024c); Lv et al. (2024); Yao et al. (2024); Sun et al..

041 To address the issue of test data contamination, a variety of training data detection methods have  
042 been proposed Shi et al.; Zhang et al. (2024b;a); Golchin & Surdeanu (2023); Jacovi et al.. These  
043 approaches typically frame the task as a binary classification problem, aiming to distinguish between  
044 contaminated data (i.e., data that has been seen by large language models during training) and clean  
045 data (i.e., data not present in the pre-training set) within a potentially contaminated dataset. The  
046 identified clean data can then be used for reliable evaluation of LLMs, mitigating the impact of  
047 contamination on LLM evaluation.

048 However, due to the black-box nature of LLMs, even state-of-the-art detection models struggle to  
049 perfectly separate contaminated from clean data. That means a significant proportion of contaminated  
050 samples may be misclassified as clean, i.e., false positives, leading to residual contamination in  
051 the selected evaluation set and undermining the reliability of model evaluation (as demonstrated  
052 in the Experiment section 5.4). If the proportion of false positives can be controlled below a user-  
053 specified threshold, residual contamination can be effectively reduced. From the perspective of  
statistical hypothesis testing, this problem can be formulated as a false discovery rate (FDR) control

problem. Classical approaches, such as the Benjamini–Hochberg (BH) procedure Benjamini & Hochberg (1995); Ferreira & Zwinderman (2006), can be employed to achieve this control. While these FDR-controlled methods exhibit desirable statistical properties Benjamini & Hochberg (1995); Benjamini & Yekutieli (2001), they often overlook another critical objective in training data detection: maximizing the amount of clean data identified, also known as detection power. Insufficient detection power may result in only a small number of clean samples being retained, thereby compromising the representativeness and robustness of subsequent evaluation. This challenge motivates a key question: Can we achieve the FDR control while maximizing detection power for training data detection?

To settle this problem, we propose TD4Eval, a training data detection framework designed for reliable LLM evaluation, with a dual focus on FDR control and power maximization. Specifically, we introduce a novel fusion strategy that integrates multiple detection techniques, such as PPL Li (2023), Min-k Shi et al., and Min-k++ Zhang et al. (2024b), into the classical BH. Our approach proceeds in three steps: first, test statistics are extracted from each detection method for every candidate sample to compute individual p-values. Then, due to data heterogeneity, i.e., detectors may exhibit different performance across datasets, we propose a rejection-count-based adaptive weighting strategy that adaptively learns the relative contribution of each detector. Based on these weights, we integrate multiple complementary detectors through the weighted Cauchy combination. Finally, we apply the BH procedure to control the overall FDR with power maximization.

From a theoretical perspective, due to data heterogeneity, we adopt a data-driven weighting scheme instead of fixed weights. However, since these weights are estimated from the same sample that generates the p-values, they become stochastically dependent on the underlying test statistics, rendering previous theoretical results based on fixed weights inapplicable (Bates et al., 2023; Wu et al., 2023; Long et al., 2023). To address this challenge, we establish the convergence of data-driven weights and extend the analysis for converged weights. The new theoretical results show TD4Eval achieves asymptotic optimality in controlling FDR and maintaining high power.

Finally, we validate the effectiveness of TD4Eval through experiments on both real-world datasets and practical evaluation benchmark. Specifically, we conduct experiments on real datasets WikiMIA Shi et al., arXivTection Duarte et al. (2024), BBC Real-Time Li et al. (2024), and MIMIR (Duan et al.), and find that TD4Eval achieves an average improvement of 30% in FDR performance compared to the SOTA, demonstrating its effectiveness in controlling false positives. In the real-world benchmark evaluation, we construct a contaminated setting by fine-tuning LMMs on the 4 classical LLM evaluation benchmarks. The results demonstrate that TD4Eval successfully identifies clean data with a controlled FDR, effectively mitigating the impact of data contamination and preserving the reliability of the model evaluation.

- To the best of our knowledge, we are the first to propose controlling the FDR while maximizing power for detecting clean data under data contamination. This effectively mitigates the impact of contaminated data and enhances the reliability of the model evaluation.
- We introduce TD4Eval, a training data detection method that offers theoretical guarantees for FDR control and power maximization.
- We validate the effectiveness of our approach on real-world datasets and demonstrate its capability to support reliable model evaluation.

## 2 RELATED WORKS

**Data Contamination.** Data contamination has been extensively studied in the literature Mann et al. (2020); Magar & Schwartz (2022); Deng et al. (2024); Golchin & Surdeanu (2024), where training data may inadvertently include evaluation benchmark data, leading to unreliable evaluation results. As such, assessing the potential leakage of benchmark data into pretraining corpora is essential for trustworthy model evaluation Dong et al. (2024); Dekoninck et al. (2024); Wang et al.; Jain et al.; Oren et al. (2023); Golchin & Surdeanu. In fact, the problem of data contamination can, to some extent, be viewed as a specific instance of Membership Inference Attacks (MIA) Das et al. (2024); Duan et al. (2024), which aim to determine whether a given data point was part of a model’s training set. Motivated by this connection, several recent works have approached training data detection in LLMs from the perspective of MIA. For example, Shi et al. hypothesize that clean data is more likely to contain outlier tokens that result in significantly higher loss values. Based on this observation, they propose the Min-K% method, which identifies contaminated data by analyzing the top-k token

108 log probabilities. Building on this, Zhang et al. (2024b) introduce Min-K%++, grounded in the  
 109 theoretical insight that training samples tend to correspond to local maxima of the model’s likelihood  
 110 function along each input dimension. Furthermore, Zhang et al. (2024a) observe that after fine-tuning  
 111 the model with a small set of unseen data, the perplexity of LLMs shifts differently for contaminated  
 112 versus clean data. Leveraging this behavior, they propose the FSD method.  
 113

114 **FDR Control.** Reformulating the training data detection problem as a multiple testing problem, the  
 115 proportion of false positives among the clean data corresponds to the false discovery rate (FDR). To  
 116 ensure that the FDR remains below a user-specified threshold, extensive research in the statistical  
 117 literature has focused on FDR control. It serves as a powerful tool for reliably identifying true  
 118 positives while limiting excessive false discoveries Benjamini & Hochberg (1995); Benjamini &  
 119 Yekutieli (2001), which is crucial in a wide range of application domains, such as genomics Storey &  
 120 Tibshirani (2003) and healthcare Genovese et al. (2002). For example, Zhang et al. (2022b) investigate  
 121 strategies to improve model selection under FDR control, while Bates et al. (2023) introduce a method  
 122 to control the FDR for a fixed novelty detection model. However, their work does not consider the  
 123 theoretical guarantees under statistical power and data-driven weights.  
 124

125 In contrast to previous work, we argue that simultaneously controlling the FDR and maximizing  
 126 detection power on clean data is critical for training data detection, as residual contamination can  
 127 undermine the reliability of model evaluations. Therefore, we propose TD4Eval, designed to achieve  
 128 rigorous and reliable evaluations of LLMs. In addition, we establish theoretical guarantees for both  
 129 FDR control and statistical power, highlighting the theoretical validity of our method.  
 130

### 3 PROBLEM DEFINITIONS

131 Suppose we are given a dataset in which a portion of the data is contaminated. The dataset consists  
 132 of  $n$  samples, denoted by  $Z_1, Z_2, \dots, Z_n$ , and indexed by  $\mathcal{D}_{\text{total}} = [n] = \{1, 2, \dots, n\}$ . Each sample  
 133 belongs either to the contaminated data or the clean data. Specifically, if a data sample has been seen  
 134 during the training process of a LLM, it is considered **contaminated**; otherwise, it is considered  
 135 **clean**. Accordingly, we define two disjoint index sets:  $\mathcal{D}_{\text{con}} \subseteq \mathcal{D}_{\text{total}}$ : indices of contaminated data,  
 136  $\mathcal{D}_{\text{clean}} = \mathcal{D}_{\text{total}} \setminus \mathcal{D}_{\text{con}}$ : indices of clean data.  
 137

138 The goal of training data detection is to estimate the set of clean data, denoted by  $\hat{\mathcal{S}} \subseteq \mathcal{D}_{\text{total}}$ , which  
 139 can be used to support reliable LLM evaluation. This task can be formulated as a classification  
 140 problem: determining whether a given sample  $Z_i$  belongs to the  $\mathcal{D}_{\text{con}}$  or  $\mathcal{D}_{\text{clean}}$ . The decision is based  
 141 on a detection score  $S_i$ , where, in general, lower scores are assumed to indicate a higher likelihood  
 142 that the sample was seen during training. Formally, the prediction function is defined as:  
 143

$$h(Z_i) = \begin{cases} \text{contaminated data} & \text{if } S_i < t, \\ \text{clean data} & \text{if } S_i \geq t, \end{cases} \quad (1)$$

144 where  $t$  is a threshold determined based on the distribution of detection scores.  
 145

146 To compute such scores, many methods have been proposed, such as Min-K%, which uses the  
 147 average probability of the  $k\%$  outlier tokens with the lowest predicted probabilities. While these  
 148 methods can distinguish clean and contaminated data to some extent, the black-box nature of LLMs,  
 149 including the inaccessibility of their full pretraining data and model architecture, makes this task  
 150 particularly challenging. As a result, even SOTA detection methods often yield clean data that contain  
 151 a significant proportion of contaminated data, thereby undermining the reliability of evaluation.  
 152

153 In this paper, we adopt a statistical perspective and aim to control the proportion of contaminated data  
 154 in selected set  $\hat{\mathcal{S}}$ . Specifically, for each sample  $i \in \mathcal{D}_{\text{total}}$ , we consider the following hypothesis test:  
 155

$$\begin{cases} \mathbb{H}_0 : \text{Sample } i \text{ is from contaminated data,} \\ \mathbb{H}_1 : \text{Sample } i \text{ is from clean data} \end{cases} \quad (2)$$

156 Our objective is to control the FDR of  $\hat{\mathcal{S}}$  to be below a user-specified threshold  $\alpha$ , while simultaneously  
 157 maximizing the power of the detection. These quantities are formally defined as:  
 158

$$\text{FDR} := \mathbb{E} \left[ \frac{|\hat{\mathcal{S}} \cap \mathcal{D}_{\text{con}}|}{|\hat{\mathcal{S}}| \vee 1} \right] \quad \text{and} \quad \text{Power} := \mathbb{E} \left[ \frac{|\hat{\mathcal{S}} \cap \mathcal{D}_{\text{clean}}|}{|\mathcal{D}_{\text{clean}}| \vee 1} \right]. \quad (3)$$

## 162 4 METHODS

164 In this section, we introduce TD4Eval, a method for detecting non-training data with rigorous  
 165 FDR control and power maximization, enabling reliable evaluation of LLMs. Specifically, we first  
 166 formalize the training data detection task as a multiple hypothesis testing problem and review the  
 167 classical Benjamini–Hochberg (BH) Benjamini & Hochberg (1995) procedure for FDR control.  
 168 Building upon BH, we then propose a cauchy fusion that integrates existing training data detection  
 169 methods to maximize detection power. Finally, we provide theoretical guarantees for the TD4Eval.

### 170 4.1 BH PROCEDURE

171 To control the FDR, we formulate the training data detection task as a multiple hypothesis testing  
 172 problem. Specifically, for each test sample  $Z_i$ , we test the null hypothesis,  
 173

$$174 H_0^{(i)} : \text{“Sample } Z_i \text{ is from the contaminated data”}.$$

175 By computing a p-value  $p_i$  for each sample, we obtain a collection of  $n$  hypotheses  $\{H_0^{(i)}\}_{i=1}^n$ , one  
 176 for each test sample. This formulation enables the application of classical multiple testing procedures  
 177 to determine which hypotheses to reject.

178 To obtain the p-value, we first compute a detection score  $S_i$  for each sample  $Z_i$  using a given  
 179 detection method. Let  $S_{\text{ref}}$  denote the contaminated data detection score distribution. Although the  
 180 true distribution of contaminated data is not directly accessible, it can be approximated by collecting  
 181 samples from commonly used pretraining sources, such as Wikipedia, that are from the same domain  
 182 and were published prior to the model’s release date. For example, WIKIMIA Shi et al. considers  
 183 Wikipedia articles created before 2017 as contaminated data, because many pretrained models,  
 184 including LLaMA and GPT-NeoX, were released after 2017 and incorporate Wikipedia dumps into  
 185 their pretraining corpora. The p-value for sample  $Z_i$  is then defined as:

$$186 p_i = \mathbb{P}_{S \sim S_{\text{ref}}}(S \leq S_i). \quad (4)$$

187 BH procedure is a classical method in multiple hypothesis testing, which aims to control the error  
 188 rate by identifying a data-dependent threshold such that FDR is bounded by a target level  $\alpha \in (0, 1)$ .  
 189 Specifically, given a set of p-values  $\{p_i\}_{i=1}^n$ , we first sort them in ascending order:  $p_{(1)} \leq p_{(2)} \leq \dots \leq p_{(n)}$ , and then find the largest index:  
 190

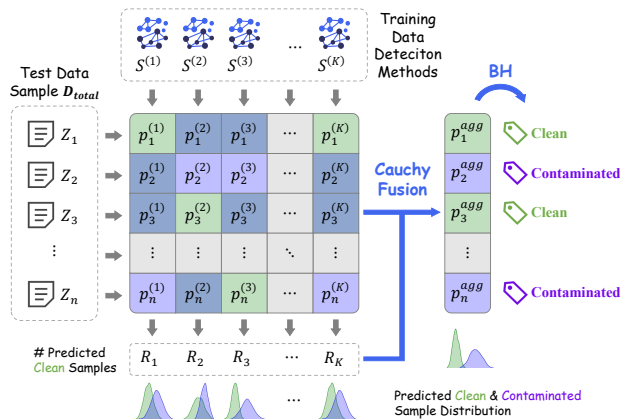
$$192 m = \max \left\{ j \in [n] : p_{(j)} \leq \frac{j\alpha}{n} \right\}, \quad (5)$$

193 The resulting BH threshold is then given by  $t_{\text{BH}} = \frac{m\alpha}{n}$ . Finally, all p-values smaller than  $t_{\text{BH}}$   
 194 are considered statistically significant, leading to the rejection of the null hypothesis  $H_0$ , and the  
 195 corresponding samples are identified as clean data. The final  $\hat{S}$  can be represent as:  
 196

$$197 \hat{S} = \{Z_j \in \mathcal{D}_{\text{total}} : p_j < t_{\text{BH}}\}. \quad (6)$$

### 198 4.2 TD4EVAL

200 While the BH procedure effectively  
 201 controls the FDR, it overlooks the  
 202 goal of maximizing statistical power.  
 203 This can result in only a small num-  
 204 ber of clean samples being detected,  
 205 thereby compromising the comprehen-  
 206 siveness of model evaluation. Re-  
 207 cent advances in training data detec-  
 208 tion have introduced various scoring  
 209 methods (e.g., Min-K Shi et al., Min-  
 210 K++ Zhang et al. (2024b), etc.), each  
 211 capturing different aspects of the data.  
 212 These methods provide complemen-  
 213 tary information, which motivates the  
 214 idea of combining multiple statistics  
 215 to construct a more powerful p-value.  
 The framework is shown in Figure 1.



216 Figure 1: The framework of TD4Eval.

Suppose we have a set of training data detection methods, each associated with a score function  $S^{(1)}, \dots, S^{(K)}$ . The corresponding p-values based on these score functions are denoted as  $\{p_j^{(1)}\}_{j \in [n]}, \dots, \{p_j^{(K)}\}_{j \in [n]}$ , respectively. Since the performance of each detection method may vary, we aim to better integrate the information from different models by assigning them appropriate weights. Intuitively, the more non-training data points a method successfully identifies (i.e., rejects the null hypothesis  $H_0$ ), the more it contributes to the overall power (Zhang et al., 2022b). Therefore, we compute the weight of each method  $S^{(k)}$  based on the number of rejections it makes under a controlled FDR:

$$R_k = \left| \left\{ Z_i \in \mathcal{D}_{\text{total}} : p_i^{(k)} \leq t_{\text{BH}}^{(k)} \right\} \right|, \quad w_k = \frac{R_k}{\sum_{j=1}^K R_j}. \quad (7)$$

Here,  $t_{\text{BH}}^{(k)}$  is the rejection threshold determined by the BH procedure over  $\{p_j^{(k)}\}_{j \in [n]}$ . Inspired by Liu & Xie (2020), we map the individual p-value to the Cauchy space and compute a weighted sum:

$$T_i = \sum_{k=1}^K w_k \cdot \tan \left[ \left( 0.5 - p_i^{(k)} \right) \pi \right]. \quad (8)$$

The reason why we choose the Cauchy distribution is that it is a heavy-tailed distribution. This implies that when an individual p-value is very small (i.e., highly significant), its corresponding Cauchy-transformed value becomes extremely large (approaching infinity). Such behavior allows the combined statistic  $T_i$  to be dominated by the most significant evidence among the individual tests, thereby increasing the sensitivity to strong signals while maintaining robustness under  $H_0$ .

The combined test statistic  $T_i$  approximately follows a standard Cauchy distribution. To map it back to the p-value space, we apply the inverse Cauchy transformation. The resulting aggregated p-value can then be used for FDR control. Specifically, the final p-value is computed as:

$$p_i^{\text{agg}} = \frac{1}{2} - \frac{1}{\pi} \arctan(T_i). \quad (9)$$

The combined p-value  $p_i^{\text{agg}}$  can then be used in the BH procedure to control the overall FDR and maximize power. The final threshold  $t$  is defined as:

$$t_{\text{final}} = \frac{\alpha}{n} \max \left\{ j \in [n] : p_{(j)}^{\text{agg}} \leq \frac{j\alpha}{n} \right\}, \quad (10)$$

where  $p_{(j)}^{\text{agg}}$  denotes the  $j$ th smallest value among the set  $\{p_i^{\text{agg}}\}_{i \in [n]}$ . The final  $\hat{\mathcal{S}}$  can be represent as:

$$\hat{\mathcal{S}} = \{Z_j \in \mathcal{D}_{\text{total}} : p_j < t_{\text{final}}\}. \quad (11)$$

### 4.3 THEORETICAL GUARANTEE

In this section, we theoretically prove that TD4Eval can effectively control the FDR while maximizing statistical power. We begin by presenting two key lemmas, which form the theoretical foundation for establishing the FDR control guarantee of the TD4Eval procedure. Specifically, we first characterize the statistical properties of the aggregated p-values used in TD4Eval. Based on these properties, we then demonstrate the effectiveness of TD4Eval in controlling the FDR.

**Lemma 1.** Bates et al. (2023) Under the null hypothesis  $H_0$ , suppose the score  $S_i^{(k)}$  is drawn from the same distribution as the reference data, i.e.,  $S_i^{(k)} \sim \mathcal{S}_{\text{ref}}^{(k)}$ , and the p-value is defined as  $p_i^{(k)} = \mathbb{P}_{S \sim \mathcal{S}_{\text{ref}}^{(k)}}(S \leq S_i^{(k)})$ . Then, under  $H_0$ , the p-value  $p_i^{(k)}$  follows a uniform distribution:  $p_i^{(k)} \sim \text{Uniform}[0, 1]$ .

Lemma 1 has been proved by Bates et al. (2023). Building on Lemma 1, consider the p-values  $p_i^{(1)}, \dots, p_i^{(K)}$  computed from different training data detectors. Each of these p-values satisfies,

$$p_i^{(k)} \sim \text{Uniform}[0, 1] \quad \text{under the null hypothesis } H_0.$$

Then, the Cauchy-aggregated p-values  $\{p_i^{\text{agg}}\}_{i \in [n]}$  can be approximately uniformly distributed under fixed weights (Liu & Xie, 2020), and this result has been extended to various structures (Wu et al.,

270 2023; Long et al., 2023). However, as we use a rejection-count-based adaptive weighting strategy  
 271 that adaptively learns the relative contribution of each detector, these data-driven weights introduce  
 272 additional theoretical challenges against fixed weights. Specifically, the estimated weights are  
 273 computed from the same sample that generates the p-values, so they are stochastically dependent on  
 274 the underlying test statistics. To address this issue, we first establish Lemma 2, which demonstrates  
 275 that the data-driven weights converge to fixed constants. We then present Lemma 3, which ensures  
 276 that the aggregated p-values preserve uniformity.

277 **Lemma 2** (Convergence of the weights for TD4Eval). *Consider  $K$  detection methods, each with score  
 278 function  $S^{(1)}, \dots, S^{(K)}$ . For each method  $k$ , let p-values on the total dataset  $\mathcal{D}_{\text{total}}$  be  $\{p_i^{(k)}\}_{i=1}^n$ .  
 279 Apply the BH procedure at level  $\alpha$  separately to each method, producing the rejection threshold  $t_{\text{BH}}^{(k)}$   
 280 and the number of rejections  $R_k = |\{Z_i \in \mathcal{D}_{\text{total}} : p_i^{(k)} \leq t_{\text{BH}}^{(k)}\}|$ . Define the normalized data-driven  
 281 weights  $w_k = \frac{R_k}{\sum_{j=1}^K R_j}$ . Then, there exist deterministic constants  $(w_1^*, \dots, w_K^*)$  with  $\sum_{k=1}^K w_k^* = 1$   
 282 such that  $w_k \xrightarrow{\text{a.s.}} w_k^*$  for each  $k = 1, \dots, K$ .*

283 **Lemma 3** (Uniformity of aggregated p-values in TD4Eval). *Let  $p_i^{(1)}, \dots, p_i^{(K)}$  be the p-values  
 284 corresponding to a given sample  $i$ , each satisfying  $p_i^{(k)} \sim \text{Uniform}[0, 1]$  under the null hypothesis  
 285  $H_0$ . We have that the aggregated p-value  $p_i^{\text{agg}}$  is uniformly distributed on  $[0, 1]$  under  $H_0$ .*

286 **Remark 1.** *A detailed theoretical analysis supporting Lemmas 2 and 3 is provided in Appendix 9.  
 287 In addition, we empirically evaluate the distribution of aggregated p-values  $p_i^{\text{agg}}$  under the null  
 288 hypothesis on real datasets. The results show that the aggregated p-values are uniformly distributed  
 289 on  $[0, 1]$ , which provides empirical evidence supporting the validity of Lemma 3.*

290 Based on the result of Lemma 3, we have the following theorems:

291 **Theorem 1** (FDR Control of TD4Eval). *Suppose we are given a set of training data detection methods,  
 292 each associated with a score function  $S^{(1)}, \dots, S^{(K)}$ . Let the corresponding p-values be defined as  
 293  $\{p_j^{(1)}\}_{j \in [n]}, \dots, \{p_j^{(K)}\}_{j \in [n]}$ , where each p-value is computed as  $p_i^{(k)} = \mathbb{P}_{S \sim S_{\text{ref}}^{(k)}}(S \leq S_i^{(k)})$ . Then,  
 294 the TD4Eval procedure controls the FDR at level  $\alpha$ , i.e.,*

$$295 \text{FDR} := \mathbb{E} \left[ \frac{|\hat{\mathcal{S}} \cap \mathcal{D}_{\text{con}}|}{|\hat{\mathcal{S}}| \vee 1} \right] \leq \alpha. \quad (12)$$

300 **Theorem 2** (Asymptotic Power Consistency of TD4Eval). *Assume that for each  $k \in [K]$  and  
 301  $Z_j \in \mathcal{D}_{\text{clean}}$ ,  $\Pr(p_j^{(k)} \leq c) \geq 1 - \delta$  where  $\delta = o(\sqrt{\log n/n})$  and  $c$  is a constant, and the density  
 302 function of  $p_j^{\text{agg}}$  for  $Z_j \in \mathcal{D}_{\text{clean}}$  has an upper bound  $C_f > 0$ , we have,*

$$303 \text{Power} := \mathbb{E} \left[ \frac{|\hat{\mathcal{S}} \cap \mathcal{D}_{\text{clean}}|}{|\mathcal{D}_{\text{clean}}| \vee 1} \right] \geq 1 - C \sqrt{\log n/n}. \quad (13)$$

308 The assumption in Theorem 2 is standard for proving power consistency (Genovese et al., 2002;  
 309 Weinstein et al., 2023). Specifically, we show that the power of TD4Eval is lower bounded by  
 310  $1 - C \sqrt{\log n/n}$ , where  $C > 0$  is a constant depending on the testing level, the null proportion, and  
 311 certain distributional characteristics. Consequently, as  $n \rightarrow \infty$ , the power converges to 1. Through  
 312 Theorems 1 and 2, we demonstrate that TD4Eval achieves asymptotic optimality in controlling the  
 313 FDR while maintaining high statistical power. Details will be presented in Appendix 10.

## 314 5 EXPERIMENTS

315 In this section, we first introduce the baselines, datasets, and experimental setup. We then present the  
 316 experimental results to demonstrate the effectiveness of our model. The code is available for review<sup>1</sup>.

### 317 5.1 SETUP

318 **Baselines** We select several baselines from prior work on training data detection, including PPL  
 319 Li (2023), Lowercase Carlini et al. (2021), Zlib Carlini et al. (2021), Grad Hu et al., Min-K% Shi  
 320 et al., and Min-K%++ Zhang et al. (2024b). In addition, to assess the effectiveness of our adaptive  
 321 weighting strategy, we construct three TD4Eval variants: BH-Average, BH-Random, and BH-Max.  
 322 Detailed descriptions are provided in the Appendix 11.1.

323 <sup>1</sup><https://anonymous.4open.science/r/TD4Eval-0D60/>

Table 1: The detection performance on three datasets. FDR (lower is better), Power (higher is better), ACC (higher is better), AUC (higher is better). **Bold** indicates the best result per model. For TD4Eval, we report the mean and standard deviation across ten independent runs.

| Method         | WikiMIA      |              |              |              |              |              | arXivTection |              |              |              |              |              | BBC Real Time |              |              |              |              |              |              |              |              |              |              |              |
|----------------|--------------|--------------|--------------|--------------|--------------|--------------|--------------|--------------|--------------|--------------|--------------|--------------|---------------|--------------|--------------|--------------|--------------|--------------|--------------|--------------|--------------|--------------|--------------|--------------|
|                | Pythia-2.8B  |              |              | LLaMA-13B    |              |              | Pythia-2.8B  |              |              | LLaMA-13B    |              |              | Pythia-2.8B   |              |              | LLaMA-13B    |              |              |              |              |              |              |              |              |
|                | FDR↓         | Power↑       | ACC↑         | AUC↑         | FDR↓         | Power↑       | ACC↑         | AUC↑         | FDR↓         | Power↑       | ACC↑         | AUC↑         | FDR↓          | Power↑       | ACC↑         | AUC↑         | FDR↓         | Power↑       | ACC↑         | AUC↑         |              |              |              |              |
| PPL            | 0.141        | 0.980        | 0.913        | 0.983        | 0.145        | 1.000        | 0.919        | 0.999        | 0.149        | 0.909        | 0.873        | 0.945        | 0.138         | 0.960        | 0.901        | 0.975        | 0.156        | <b>0.802</b> | 0.825        | 0.882        | 0.137        | 0.931        | 0.890        | 0.950        |
| Lowercase      | 0.154        | 0.926        | 0.884        | 0.954        | 0.149        | 0.999        | 0.916        | 0.996        | 0.216        | 0.615        | 0.718        | 0.825        | 0.154         | 0.832        | 0.837        | 0.922        | 0.173        | 0.694        | 0.772        | 0.853        | 0.133        | 0.928        | 0.892        | 0.949        |
| Zlib           | 0.178        | 0.768        | 0.809        | 0.880        | 0.150        | 0.959        | 0.899        | 0.977        | 0.200        | 0.580        | 0.712        | 0.822        | 0.160         | 0.819        | 0.829        | 0.909        | 0.207        | 0.550        | 0.700        | 0.797        | 0.151        | 0.832        | 0.840        | 0.903        |
| Grad           | 0.174        | 0.798        | 0.823        | 0.907        | 0.154        | 0.929        | 0.885        | 0.964        | 0.150        | 0.798        | 0.825        | 0.907        | 0.139         | 0.913        | 0.881        | 0.951        | 0.188        | 0.645        | 0.745        | 0.827        | 0.151        | 0.853        | 0.849        | 0.921        |
| Min-K%         | 0.150        | 0.982        | 0.908        | 0.982        | 0.151        | 1.000        | 0.915        | 0.999        | 0.135        | <b>0.962</b> | 0.904        | 0.972        | 0.141         | 0.995        | 0.915        | <b>0.994</b> | 0.187        | 0.656        | 0.750        | 0.833        | 0.138        | 0.910        | 0.881        | 0.942        |
| Min-K%++       | 0.145        | 0.997        | 0.918        | <b>0.993</b> | 0.150        | 1.000        | 0.915        | <b>1.000</b> | 0.148        | 0.906        | 0.872        | 0.948        | 0.137         | 0.995        | 0.917        | 0.991        | 0.167        | 0.744        | 0.795        | 0.866        | 0.133        | 0.935        | 0.894        | 0.950        |
| <b>TD4Eval</b> | <b>0.101</b> | <b>0.999</b> | <b>0.946</b> | <b>0.993</b> | <b>0.099</b> | <b>1.000</b> | <b>0.947</b> | <b>0.998</b> | <b>0.090</b> | <b>0.942</b> | <b>0.923</b> | <b>0.973</b> | <b>0.092</b>  | <b>0.997</b> | <b>0.947</b> | <b>0.994</b> | <b>0.095</b> | <b>0.771</b> | <b>0.843</b> | <b>0.910</b> | <b>0.094</b> | <b>0.948</b> | <b>0.924</b> | <b>0.968</b> |
| (std)          | ±0.018       | ±0.001       | ±0.011       | ±0.001       | ±0.012       | ±0.000       | ±0.007       | ±0.001       | ±0.014       | ±0.010       | ±0.007       | ±0.003       | ±0.020        | ±0.002       | ±0.012       | ±0.002       | ±0.013       | ±0.017       | ±0.003       | ±0.002       | ±0.005       | ±0.002       | ±0.003       |              |

**Models and Datasets** We adopt three LLMs to evaluate our TD4Eval: Pythia-2.8B (Biderman et al., 2023), OPT-6.7B (Zhang et al. (2022a)) and LLaMA-13B (Touvron et al. (2023)). Throughout our experiments, we use the checkpoints provided by Hugging Face. As for the evaluation datasets, we employ four benchmark datasets for evaluations, including WikiMIA (Shi et al.), ArXivTection (Duarte et al. (2024)), BBC Real Time (Li et al. (2024)), MIMIR (Duan et al.). Previous works have demonstrated that model developers commonly use text content among those datasets for pre-training (Shi et al.; Duarte et al. (2024)). Detailed information is shown in [Appendix 11.2](#).

**Evaluation metrics** In this paper, we focus on two key metrics, FDR and Power (Eq. (3)), which play a crucial role in training data detection for LLM evaluation. A lower FDR and a higher Power indicate better detection performance. Additionally, we report the Accuracy (ACC) and AUC, where a higher ACC and AUC reflects more precise detection results.

**Implementation details** The detailed implementation can be found in [Appendix 11.3](#).

## 5.2 MAIN RESULT

In this section, We conduct a comprehensive comparison of various training data detection methods across three datasets and multiple language models. Table 1 summarizes the detection performance of all evaluated methods across three datasets and under multiple LLM backbones. Results for OPT-6.7B and MIMIR are provided in the [Appendix 11.4](#). The key findings are as follows: ① *TD4Eval achieves the lowest FDR across all datasets and model settings, demonstrating its strong ability to suppress false positives.* Compared to the strongest baseline, TD4Eval achieves a relative FDR reduction of up to 30–39%, indicating a substantial improvement in precision when identifying clean data. ② *TD4Eval maintains competitive or superior detection power in most settings.* It achieves near-perfect power on two datasets and performs robustly on the third, showing that it can effectively recall clean samples while maintaining low FDR. ③ *TD4Eval consistently achieves the highest overall accuracy across different datasets and models.* This reflects its comprehensive effectiveness in both minimizing false detections and correctly identifying clean data, which is crucial for downstream applications.

### 5.3 THE ANALYSIS OF TD4EVAL

**Effect of Cauchy Fusion.** We adapt a weighted Cauchy fusion strategy as defined in Eq. (8) and Eq. (9). In this section, we evaluate its effectiveness from two perspectives. First, we assess the benefit of fusion itself. To this end, we remove the fusion module and directly compute the p-values from individual detection methods. We then apply the BH procedure described in Section 4.1 to control the FDR, resulting in a set of baselines denoted as BH-XX, where XX indicates the name of the detection method. Second, we examine the impact of the weighting scheme. We introduce three variants, named E shows the FDR and Power results across data findings: ① *BH-based methods effectively control FDR below the 0.15 threshold (indicated by the and robustness of the BH procedure when applied*

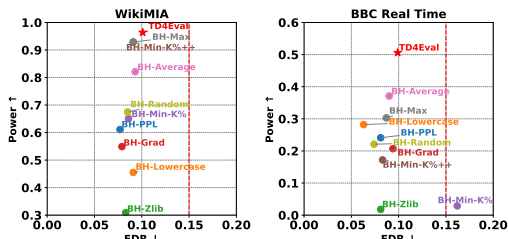


Figure 2: Ablation study results on Pythia-2.8B.

378 *all approaches, TD4Eval achieves the highest Power while keeping FDR within the acceptable*  
 379 *range. Compared to BH-Average, BH-Random, and BH-Max, the superior performance of TD4Eval*  
 380 *highlights the benefit of our learned weighting scheme.*

382 **Effect of reference data  $S_{\text{ref}}$ .** The computation  
 383 of the p-value relies on the reference data  
 384  $S_{\text{ref}}$ . In this section, we investigate the impact  
 385 of noise in  $S_{\text{ref}}$  on TD4Eval. Specifically, we  
 386 introduce varying levels of noise into the labels  
 387 of the contaminated reference data by randomly  
 388 selecting a proportion of labels and replacing  
 389 them with labels from other classes uniformly  
 390 at random. The corresponding results for Power  
 391 and FDR are shown in Figure 3. These  
 392 results demonstrate that, compared to the base-  
 393 lines, TD4Eval consistently achieves the highest  
 394 power while effectively controlling the FDR under  
 395 different noise conditions, thereby effectively  
 396 enhancing the robustness of detection.

396 **Effect of  $\alpha$ .** To investigate the impact of the  
 397 FDR control threshold  $\alpha$  on model performance,  
 398 we vary  $\alpha$  from 0.02 to 0.18 and compute the  
 399 corresponding FDR and Power for each method.  
 400 Each subplot in Figure 4 presents results on a  
 401 different dataset, and each curve corresponds  
 402 to a specific metric. To clearly visualize the  
 403 FDR constraint, we also include a dashed line  
 404 representing the target threshold ( $y = \alpha$ ). A  
 405 model is considered to successfully control the  
 406 FDR if its corresponding FDR curve remains  
 407 below this line. As  $\alpha$  increases, the observed  
 408 FDR (blue curve) consistently remains below the target threshold (dashed line  $y = \alpha$ ) across all  
 409 datasets, demonstrating that TD4Eval successfully controls the FDR within the specified bounds.  
 410 This indicates that the TD4Eval is statistically valid and reliable across a wide range of  $\alpha$  values.

410 **Analysis of learning weight  $w_i$ .** To further ex-  
 411 amine the effectiveness of our weighted fusion  
 412 strategy, we visualize the learned weights as-  
 413 signed to each method across different datasets,  
 414 as shown in Figure 5. The pie charts correspond  
 415 to the datasets WikiMIA, arXivTection. Each  
 416 segment represents the weight of a base method  
 417 in the final fusion. We observe that methods with  
 418 stronger performance (as reported in the table  
 419 1) tend to receive larger weights. For instance,  
 420 Min-K%++ and Min-K% consistently receive  
 421 higher weights across all datasets, while Grad  
 422 and Zlib are assigned smaller weights. This  
 423 alignment between performance and weighting  
 424 indicates that our fusion mechanism is capable of  
 425 effectively distinguishing the power of each method, and integrates them in a power-aware manner.

#### 425 5.4 THE APPLICATION OF TD4EVAL

426 In this section, we explore the practical application of TD4Eval to assess whether it can mitigate  
 427 the impact of test data contamination on model evaluation. Since existing data contamination  
 428 evaluation benchmarks do not support model evaluation, we construct a synthetic contaminated  
 429 setting. Specifically, we fine-tune an LLM using a subset of the evaluation data, thereby intentionally  
 430 introducing contamination. We then apply training data detection methods to identify the clean data,  
 431 and examine the evaluation results. Since each training data detection method selects a different clean  
 432 benchmark dataset, comparing their absolute scores in different clean sets would be unfair. Therefore,

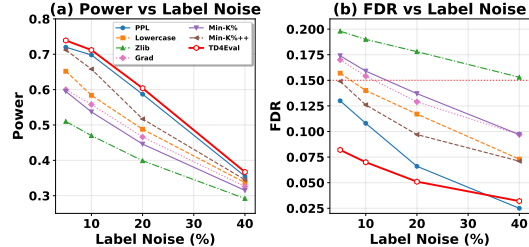


Figure 3: The results for Pythia-2.8B on the BBC dataset under different levels of label noise. These results demonstrate that, compared to the baselines, TD4Eval consistently achieves the highest power while effectively controlling the FDR under different noise conditions. This result also indicates that the dynamic weighting strategy in our TD4Eval can integrate the strengths of multiple detectors, thereby effectively enhancing the robustness of detection.

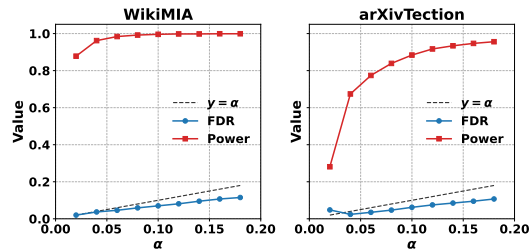


Figure 4: The impact of  $\alpha$  on Pythia-2.8B.

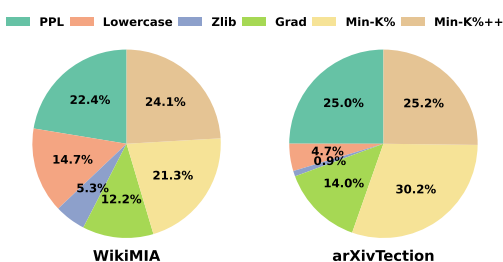


Figure 5: Learned weights for each method in the TD4Eval on Pythia-2.8B.

432  
 433 Table 2: Impact of different detection methods on LLM Evaluation, SRCC metric measures whether  
 434 a detector can effectively remove contaminated data and thereby preserve ranking consistency in  
 435 model evaluation; values closer to 1 indicate higher consistency. The **Contaminated** row reports the  
 436 **benchmark results of the contaminated models without applying any training data detection methods.**

| Method         | Simple QA    |              |              |              | GPQA         |              |              |              | TruthfulQA   |              |              |              | ARC-C        |              |              |              |
|----------------|--------------|--------------|--------------|--------------|--------------|--------------|--------------|--------------|--------------|--------------|--------------|--------------|--------------|--------------|--------------|--------------|
|                | LLaMA-3.1-8B |              | Mistral-7B   |              | LLaMA-3.1-8B |              | Mistral-7B   |              | LLaMA-3.1-8B |              | Mistral-7B   |              | LLaMA-3.1-8B |              | Mistral-7B   |              |
|                | FDR↓         | SRCC↑        |
| Contaminated   | -            | 0.657        | -            | 0.500        | -            | 0.143        | -            | 0.886        | -            | 0.657        | -            | 0.429        | -            | 0.643        | -            | 0.464        |
| PPL            | 0.134        | 0.886        | 0.223        | 0.810        | 0.056        | 0.771        | 0.148        | 0.829        | 0.125        | 0.714        | 0.178        | 0.657        | 0.145        | 0.786        | 0.124        | 0.893        |
| Lowercase      | 0.135        | 0.829        | 0.248        | 0.833        | 0.045        | 0.829        | 0.113        | 0.943        | 0.128        | 0.829        | 0.171        | 0.829        | 0.182        | 0.750        | 0.151        | 0.750        |
| Zlib           | 0.125        | 0.829        | 0.234        | 0.833        | 0.086        | 0.600        | 0.227        | 0.714        | 0.120        | 0.829        | 0.165        | 0.657        | 0.125        | 0.929        | 0.101        | 0.964        |
| Grad           | 0.116        | <b>1.000</b> | 0.108        | 0.929        | 0.056        | 0.600        | 0.179        | 0.886        | 0.128        | 0.657        | 0.198        | 0.771        | 0.109        | 0.964        | 0.075        | <b>1.000</b> |
| Min-K%         | 0.139        | 0.943        | 0.199        | 0.810        | 0.054        | 0.657        | 0.142        | 0.886        | 0.133        | 0.715        | 0.208        | 0.829        | 0.134        | 0.857        | 0.113        | 0.893        |
| Min-K%++       | 0.118        | <b>1.000</b> | 0.172        | 0.857        | 0.031        | 0.829        | 0.105        | 0.943        | 0.112        | 0.829        | 0.147        | 0.943        | 0.135        | 0.857        | 0.105        | 0.964        |
| <b>TD4Eval</b> | <b>0.096</b> | <b>1.000</b> | <b>0.025</b> | <b>1.000</b> | <b>0.025</b> | <b>0.943</b> | <b>0.057</b> | <b>1.000</b> | <b>0.074</b> | <b>1.000</b> | <b>0.087</b> | <b>1.000</b> | <b>0.061</b> | <b>1.000</b> | <b>0.070</b> | <b>1.000</b> |

440 we focus on the consistency of the ranking instead. We argue that a reliable detection method should  
 441 preserve the relative ranking of models as observed on the clean benchmark.

442 More concretely, we consider four widely used LLM evaluation benchmarks: SimpleQA Wei et al.  
 443 (2024), GPQA Rein et al. (2023), TruthfulQA Lin et al. (2022), and ARC-C Clark et al. (2018).  
 444 Detailed descriptions of these benchmarks are provided in the [Appendix 12.1](#). We evaluate eight  
 445 models on these four benchmarks: LLaMA-3-70B Grattafiori et al. (2024), GPT-4o-mini Hurst et al.  
 446 (2024), o1-mini Jaech et al. (2024), Gemini-1.5-Flash Team et al. (2024), Mistral-7B Jiang (2024),  
 447 Claude-3-Haiku Anthropic (2024), LLaMA-3.1-8B Meta AI (2024a), and LLaMA-3.2-3B Meta AI  
 448 (2024b). The rankings of these models on the benchmarks serve as the ground truth for evaluating  
 449 model performance under clean conditions. To simulate contamination, we randomly select 50% of  
 450 the benchmarks to fine-tune certain LLMs (specifically, LLaMA-3.1-8B and Mistral-7B), thereby  
 451 introducing artificial contamination. The detailed fine-tuning setup is provided in [Appendix 12.2](#).  
 452 To evaluate the effectiveness of training data detection, we apply various detection methods to filter  
 453 out contaminated samples and retain only clean evaluation data. We then compare the relative  
 454 rankings of the eight models based on their performance. The closer these rankings are to the  
 455 clean-condition ground truth, the more effective the detection method. For quantitative evaluation, we  
 456 adopt Spearman’s Rank Correlation Coefficient (SRCC) Sedgwick (2014) as the consistency metric;  
 457 values closer to 1 indicate that the detection method more effectively preserves reliable evaluation of  
 458 LLMs. The experimental results are summarized in Table 2.

459 From the table, we have the following findings: ① *Data contamination severely compromises fair*  
 460 *model evaluation.* From the **Contaminated** row, we observe that after introducing contamination,  
 461 the performance rankings of the affected models deviate substantially from the clean-condition  
 462 ground truth. This demonstrates that contamination can lead to misleading conclusions about their  
 463 true capabilities. ② *Existing training data detection methods are helpful but insufficient.* While  
 464 existing detection methods do mitigate the impact of contamination to some extent, their performance  
 465 remains unsatisfactory in terms of both the FDR and SRCC metrics. ③ *TD4Eval effectively addresses*  
 466 *data contamination in model evaluation.* Our method consistently achieves the lowest FDR among  
 467 all detection approaches. Notably, under TD4Eval, the SRCC reaches 1 across all benchmarks,  
 468 highlighting that controlling FDR is essential for minimizing the impact of data contamination and  
 469 ensuring reliable LLM evaluation. We also evaluate the effectiveness of TD4Eval under different  
 470 levels of contamination. The detailed results are provided in the [Appendix 12.3](#), which further  
 471 demonstrate that TD4Eval yields reliable LLM evaluations across varying contamination ratios.

## 472 6 CONCLUSION AND LIMITATIONS

473 In this work, we addressed the critical challenge of test data contamination in the evaluation of LLMs,  
 474 which undermines the reliability of performance assessments. We proposed TD4Eval, a principled  
 475 framework that ensures strict FDR control while maximizing the retention of clean evaluation data.  
 476 By integrating multiple detectors through the cauchy combination method and applying the BH  
 477 procedure, TD4Eval achieves both theoretical guarantees and practical effectiveness. Empirical  
 478 results across three real-world datasets demonstrate that TD4Eval consistently outperforms state-  
 479 of-the-art baselines. Our findings highlight the importance of statistically grounded approaches for  
 480 reliable LLM evaluation. The limitations will be discussed in [Appendix 13](#).

## 486 7 ETHICS STATEMENT

488 TD4Eval addresses the pressing issue of test data contamination, contributing to the growing need for  
 489 reliable evaluation of LLMs. By enabling statistically principled detection of clean evaluation data,  
 490 our framework enhances the transparency and trustworthiness of LLM benchmarking, particularly in  
 491 high-stakes applications such as education. Our research does not present ethical issues.

## 492 8 REPRODUCIBILITY STATEMENT

494 To ensure the reproducibility of our results, we provide the complete implementation of our methods,  
 495 along with all necessary code and data, on an anonymous GitHub repository. Our code is available  
 496 for review at <https://anonymous.4open.science/r/TD4Eval-0D60/>. Once our paper is accepted, we  
 497 will publicly release the code.

## 498 REFERENCES

500 Anthropic. The claude 3 model family: Opus, sonnet, and haiku. [https://www-cdn.anthropic.com/de8ba9b01c9ab7cbabf5c33b80b7bbc618857627/Model\\_Card\\_Claude\\_3.pdf](https://www-cdn.anthropic.com/de8ba9b01c9ab7cbabf5c33b80b7bbc618857627/Model_Card_Claude_3.pdf), 2024. Accessed: 2025-05-15.

503 Stephen Bates, Emmanuel Candès, Lihua Lei, Yaniv Romano, and Matteo Sesia. Testing for outliers  
 504 with conformal p-values. *The Annals of Statistics*, 51(1):149–178, 2023.

506 Yoav Benjamini and Yosef Hochberg. Controlling the false discovery rate: a practical and powerful  
 507 approach to multiple testing. *Journal of the Royal statistical society: series B (Methodological)*,  
 508 57(1):289–300, 1995.

510 Yoav Benjamini and Daniel Yekutieli. The control of the false discovery rate in multiple testing under  
 511 dependency. *Annals of statistics*, pp. 1165–1188, 2001.

512 Stella Biderman, Hailey Schoelkopf, Quentin Gregory Anthony, Herbie Bradley, Kyle O’Brien, Eric  
 513 Hallahan, Mohammad Aflah Khan, Shivanshu Purohit, USVSN Sai Prashanth, Edward Raff, et al.  
 514 Pythia: A suite for analyzing large language models across training and scaling. In *International  
 515 Conference on Machine Learning*, pp. 2397–2430. PMLR, 2023.

517 Nicholas Carlini, Florian Tramer, Eric Wallace, Matthew Jagielski, Ariel Herbert-Voss, Katherine  
 518 Lee, Adam Roberts, Tom Brown, Dawn Song, Ulfar Erlingsson, et al. Extracting training data  
 519 from large language models. In *30th USENIX security symposium (USENIX Security 21)*, pp.  
 520 2633–2650, 2021.

521 Yupeng Chang, Xu Wang, Jindong Wang, Yuan Wu, Linyi Yang, Kaijie Zhu, Hao Chen, Xiaoyuan  
 522 Yi, Cunxiang Wang, Yidong Wang, et al. A survey on evaluation of large language models. *ACM  
 523 transactions on intelligent systems and technology*, 15(3):1–45, 2024.

524 Yuxing Cheng, Yi Chang, and Yuan Wu. A survey on data contamination for large language models.  
 525 *arXiv preprint arXiv:2502.14425*, 2025.

527 Peter Clark, Isaac Cowhey, Oren Etzioni, Tushar Khot, Ashish Sabharwal, Carissa Schoenick, and  
 528 Oyvind Tafjord. Think you have solved question answering? try arc, the ai2 reasoning challenge,  
 529 2018. URL <https://arxiv.org/abs/1803.05457>.

531 Debeshee Das, Jie Zhang, and Florian Tramèr. Blind baselines beat membership inference attacks for  
 532 foundation models. *arXiv preprint arXiv:2406.16201*, 2024.

533 Jasper Dekoninck, Mark Müller, and Martin Vechev. Constat: Performance-based contamination  
 534 detection in large language models. *Advances in Neural Information Processing Systems*, 37:  
 535 92420–92464, 2024.

537 Chunyuan Deng, Yilun Zhao, Xiangru Tang, Mark Gerstein, and Arman Cohan. Investigating data  
 538 contamination in modern benchmarks for large language models. In *Proceedings of the 2024  
 539 Conference of the North American Chapter of the Association for Computational Linguistics: Human  
 Language Technologies (Volume 1: Long Papers)*, pp. 8698–8711, 2024.

540 Yihong Dong, Xue Jiang, Huanyu Liu, Zhi Jin, Bin Gu, Mengfei Yang, and Ge Li. Generalization  
 541 or memorization: Data contamination and trustworthy evaluation for large language models. In  
 542 *Findings of the Association for Computational Linguistics ACL 2024*, pp. 12039–12050, 2024.  
 543

544 Michael Duan, Anshuman Suri, Niloofar Mireshghallah, Sewon Min, Weijia Shi, Luke Zettlemoyer,  
 545 Yulia Tsvetkov, Yejin Choi, David Evans, and Hannaneh Hajishirzi. Do membership inference  
 546 attacks work on large language models? In *First Conference on Language Modeling*.  
 547

548 Michael Duan, Anshuman Suri, Niloofar Mireshghallah, Sewon Min, Weijia Shi, Luke Zettlemoyer,  
 549 Yulia Tsvetkov, Yejin Choi, David Evans, and Hannaneh Hajishirzi. Do membership inference  
 550 attacks work on large language models? *arXiv preprint arXiv:2402.07841*, 2024.  
 551

552 André V Duarte, Xuandong Zhao, Arlindo L Oliveira, and Lei Li. De-cop: Detecting copyrighted  
 553 content in language models training data. *arXiv preprint arXiv:2402.09910*, 2024.  
 554

555 William Feller. *An introduction to probability theory and its applications, Volume 2*, volume 2. John  
 556 Wiley & Sons, 1991.  
 557

558 JA Ferreira and AH Zwinderman. On the benjamini–hochberg method. 2006.  
 559

560 Leo Gao, Stella Biderman, Sid Black, Laurence Golding, Travis Hoppe, Charles Foster, Jason Phang,  
 561 Horace He, Anish Thite, Noa Nabeshima, et al. The pile: An 800gb dataset of diverse text for  
 562 language modeling. *arXiv preprint arXiv:2101.00027*, 2020.  
 563

564 Christopher R Genovese, Nicole A Lazar, and Thomas Nichols. Thresholding of statistical maps in  
 565 functional neuroimaging using the false discovery rate. *Neuroimage*, 15(4):870–878, 2002.  
 566

567 Shahriar Golchin and Mihai Surdeanu. Time travel in llms: Tracing data contamination in large  
 568 language models. In *The Twelfth International Conference on Learning Representations*.  
 569

570 Shahriar Golchin and Mihai Surdeanu. Data contamination quiz: A tool to detect and estimate  
 571 contamination in large language models. *arXiv preprint arXiv:2311.06233*, 2023.  
 572

573 Shahriar Golchin and Mihai Surdeanu. Time travel in llms: Tracing data contamination in large  
 574 language models. In *ICLR*, 2024.  
 575

576 Aaron Grattafiori, Abhimanyu Dubey, Abhinav Jauhri, Abhinav Pandey, Abhishek Kadian, Ahmad  
 577 Al-Dahle, Aiesha Letman, Akhil Mathur, Alan Schelten, Alex Vaughan, et al. The llama 3 herd of  
 578 models. *arXiv preprint arXiv:2407.21783*, 2024.  
 579

580 Zirui Hu, Yingjie Wang, Zheng Zhang, Hong Chen, and Dacheng Tao. A statistical approach  
 581 for controlled training data detection. In *The Thirteenth International Conference on Learning  
 582 Representations*.  
 583

584 Aaron Hurst, Adam Lerer, Adam P Goucher, Adam Perelman, Aditya Ramesh, Aidan Clark, AJ Os-  
 585 trow, Akila Welihinda, Alan Hayes, Alec Radford, et al. Gpt-4o system card. *arXiv preprint  
 586 arXiv:2410.21276*, 2024.  
 587

588 Alon Jacovi, Avi Caciularu, Omer Goldman, and Yoav Goldberg. Stop uploading test data in plain  
 589 text: Practical strategies for mitigating data contamination by evaluation benchmarks. In *The 2023  
 590 Conference on Empirical Methods in Natural Language Processing*.  
 591

592 Aaron Jaech, Adam Kalai, Adam Lerer, Adam Richardson, Ahmed El-Kishky, Aiden Low, Alec  
 593 Helyar, Aleksander Madry, Alex Beutel, Alex Carney, et al. Openai o1 system card. *arXiv preprint  
 594 arXiv:2412.16720*, 2024.  
 595

596 Naman Jain, King Han, Alex Gu, Wen-Ding Li, Fanjia Yan, Tianjun Zhang, Sida Wang, Armando  
 597 Solar-Lezama, Koushik Sen, and Ion Stoica. Livecodebench: Holistic and contamination free  
 598 evaluation of large language models for code. In *The Thirteenth International Conference on  
 599 Learning Representations*.  
 600

601 Fengqing Jiang. Identifying and mitigating vulnerabilities in llm-integrated applications. Master’s  
 602 thesis, University of Washington, 2024.

594 Yucheng Li. Estimating contamination via perplexity: Quantifying memorisation in language model  
 595 evaluation. *arXiv preprint arXiv:2309.10677*, 2023.  
 596

597 Yucheng Li, Frank Guerin, and Chenghua Lin. Latesteval: Addressing data contamination in language  
 598 model evaluation through dynamic and time-sensitive test construction. In *Proceedings of the*  
 599 *AAAI Conference on Artificial Intelligence*, volume 38, pp. 18600–18607, 2024.

600 Stephanie Lin, Jacob Hilton, and Owain Evans. Truthfulqa: Measuring how models mimic human  
 601 falsehoods, 2022. URL <https://arxiv.org/abs/2109.07958>.  
 602

603 Yaowu Liu and Jun Xie. Cauchy combination test: a powerful test with analytic p-value calculation  
 604 under arbitrary dependency structures. *Journal of the American Statistical Association*, 115(529):  
 605 393–402, 2020.

606 Mingya Long, Zhengbang Li, Wei Zhang, and Qizhai Li. The cauchy combination test under arbitrary  
 607 dependence structures. *The American Statistician*, 77(2):134–142, 2023.

608 Wenxi Lv, Qinliang Su, Hai Wan, Hongteng Xu, and Wencho Xu. Contamination-resilient anomaly  
 609 detection via adversarial learning on partially-observed normal and anomalous data. In *Forty-first*  
 610 *International Conference on Machine Learning*, 2024.

611 Inbal Magar and Roy Schwartz. Data contamination: From memorization to exploitation. *arXiv*  
 612 *preprint arXiv:2203.08242*, 2022.

613 Ben Mann, N Ryder, M Subbiah, J Kaplan, P Dhariwal, A Neelakantan, P Shyam, G Sastry, A Askell,  
 614 S Agarwal, et al. Language models are few-shot learners. *arXiv preprint arXiv:2005.14165*, 1:3,  
 615 2020.

616 Meta AI. Introducing llama 3.1: Our most capable models to date. [https://ai.meta.com/](https://ai.meta.com/blog/meta-llama-3-1/)  
 617 [blog/meta-llama-3-1/](https://ai.meta.com/blog/meta-llama-3-1/), 2024a. Accessed: 2025-05-15.

618 Meta AI. Llama 3.2: Revolutionizing edge ai and vision with  
 619 open, customizable models. [https://ai.meta.com/blog/](https://ai.meta.com/blog/llama-3-2-connect-2024-vision-edge-mobile-devices/)  
 620 [llama-3-2-connect-2024-vision-edge-mobile-devices/](https://ai.meta.com/blog/llama-3-2-connect-2024-vision-edge-mobile-devices/), 2024b. Accessed:  
 621 2025-05-15.

622 Yonatan Oren, Nicole Meister, Niladri S Chatterji, Faisal Ladhak, and Tatsunori Hashimoto. Proving  
 623 test set contamination in black-box language models. In *The Twelfth International Conference on*  
 624 *Learning Representations*, 2023.

625 David Rein, Betty Li Hou, Asa Cooper Stickland, Jackson Petty, Richard Yuanzhe Pang, Julien Dirani,  
 626 Julian Michael, and Samuel R. Bowman. Gpqa: A graduate-level google-proof qa benchmark,  
 627 2023. URL <https://arxiv.org/abs/2311.12022>.

628 Philip Sedgwick. Spearman’s rank correlation coefficient. *Bmj*, 349, 2014.

629 Weijia Shi, Anirudh Ajith, Mengzhou Xia, Yangsibo Huang, Daogao Liu, Terra Blevins, Danqi Chen,  
 630 and Luke Zettlemoyer. Detecting pretraining data from large language models. In *The Twelfth*  
 631 *International Conference on Learning Representations*.

632 John D Storey and Robert Tibshirani. Statistical significance for genomewide studies. *Proceedings*  
 633 *of the National Academy of Sciences*, 100(16):9440–9445, 2003.

634 John D Storey, Jonathan E Taylor, and David Siegmund. Strong control, conservative point estimation  
 635 and simultaneous conservative consistency of false discovery rates: a unified approach. *Journal of*  
 636 *the Royal Statistical Society Series B: Statistical Methodology*, 66(1):187–205, 2004.

637 Yifan Sun, Han Wang, Dongbai Li, Gang Wang, and Huan Zhang. The emperor’s new clothes in  
 638 benchmarking? a rigorous examination of mitigation strategies for llm benchmark data contamina-  
 639 tion. In *Forty-second International Conference on Machine Learning*.

640 Gemini Team, Petko Georgiev, Ving Ian Lei, Ryan Burnell, Libin Bai, Anmol Gulati, Garrett  
 641 Tanzer, Damien Vincent, Zhufeng Pan, Shibo Wang, et al. Gemini 1.5: Unlocking multimodal  
 642 understanding across millions of tokens of context. *arXiv preprint arXiv:2403.05530*, 2024.

648 Hugo Touvron, Thibaut Lavril, Gautier Izacard, Xavier Martinet, Marie-Anne Lachaux, Timothée  
 649 Lacroix, Baptiste Rozière, Naman Goyal, Eric Hambro, Faisal Azhar, et al. Llama: Open and  
 650 efficient foundation language models. *arXiv preprint arXiv:2302.13971*, 2023.

651

652 Maorong Wang, Nicolas Michel, Jiafeng Mao, and Toshihiko Yamasaki. Dealing with synthetic data  
 653 contamination in online continual learning. In *The Thirty-eighth Annual Conference on Neural  
 654 Information Processing Systems*.

655 Jason Wei, Nguyen Karina, Hyung Won Chung, Yunxin Joy Jiao, Spencer Papay, Amelia Glaese,  
 656 John Schulman, and William Fedus. Measuring short-form factuality in large language models.  
 657 *arXiv preprint arXiv:2411.04368*, 2024.

658

659 Asaf Weinstein, Weijie J Su, Małgorzata Bogdan, Rina Foygel Barber, and Emmanuel J Candes. A  
 660 power analysis for model-x knockoffs with p-regularized statistics. *The Annals of Statistics*, 51(3):  
 661 1005–1029, 2023.

662 Xiaoyang Wu, Yuyang Huo, and Changliang Zou. Multi-split conformal prediction via cauchy  
 663 aggregation. *Stat*, 12(1):e522, 2023.

664

665 Feng Yao, Yufan Zhuang, Zihao Sun, Sunan Xu, Animesh Kumar, and Jingbo Shang. Data contami-  
 666 nation can cross language barriers. *arXiv preprint arXiv:2406.13236*, 2024.

667

668 Hengxiang Zhang, Songxin Zhang, Bingyi Jing, and Hongxin Wei. Fine-tuning can help detect  
 669 pretraining data from large language models. *arXiv preprint arXiv:2410.10880*, 2024a.

670

671 Jingyang Zhang, Jingwei Sun, Eric Yeats, Yang Ouyang, Martin Kuo, Jianyi Zhang, Hao Frank Yang,  
 672 and Hai Li. Min-k%++: Improved baseline for detecting pre-training data from large language  
 673 models. *arXiv preprint arXiv:2404.02936*, 2024b.

674

675 Susan Zhang, Stephen Roller, Naman Goyal, Mikel Artetxe, Moya Chen, Shuhui Chen, Christopher  
 676 Dewan, Mona Diab, Xian Li, Xi Victoria Lin, et al. Opt: Open pre-trained transformer language  
 677 models. *arXiv preprint arXiv:2205.01068*, 2022a.

678

679 Weichao Zhang, Ruqing Zhang, Jiafeng Guo, Maarten Rijke, Yixing Fan, and Xueqi Cheng. Pre-  
 680 training data detection for large language models: A divergence-based calibration method. In  
 681 *Proceedings of the 2024 Conference on Empirical Methods in Natural Language Processing*, pp.  
 682 5263–5274, 2024c.

683

684 Yifan Zhang, Haiyan Jiang, Haojie Ren, Changliang Zou, and Dejing Dou. Automs: automatic model  
 685 selection for novelty detection with error rate control. *Advances in Neural Information Processing  
 686 Systems*, 35:19917–19929, 2022b.

687

## 9 APPENDIX A

687 TD4Eval is supported by strong statistical guarantees, enabling effective control of the FDR while  
 688 maximizing statistical power. In this section, we present two key lemmas that form the theoretical  
 689 foundation for establishing the FDR control guarantees of the TD4Eval procedure. Specifically, we  
 690 characterize the statistical properties of the aggregated p-values used in TD4Eval from both empirical  
 691 and theoretical perspectives.

692 **Lemma 1.** *Bates et al. (2023) Under the null hypothesis  $H_0$ , suppose the score  $S_i^{(k)}$  is drawn  
 693 from the same distribution as the reference data, i.e.,  $S_i^{(k)} \sim S_{ref}^{(k)}$ , and the p-value is defined  
 694 as  $p_i^{(k)} = \mathbb{P}_{S \sim S_{ref}^{(k)}}(S \leq S_i^{(k)})$ . Then, under  $H_0$ , the p-value  $p_i^{(k)}$  follows a uniform distribution:  
 695  $p_i^{(k)} \sim \text{Uniform}[0, 1]$ .*

696

697 This proof has already been established in Bates et al. (2023); we refer the reader to that work for  
 698 details. Then, we provide the detailed proof of Lemma 2. Before presenting the proof, we introduce  
 699 the BH-limit lemma, which is a well-established result in classical multiple testing theory. It states  
 700 that the ratio of rejections produced by the BH procedure to the total number of tests converges to a  
 701 constant. This result is crucial for establishing the convergence of the data-driven weights.

702 **Lemma** (BH-limit Storey et al. (2004)). *For each method  $k \in \{1, \dots, K\}$ , suppose the p-values  
 703  $\{p_i^{(k)}\}_{i=1}^n$  are i.i.d. with a mixture distribution  $F_k(t) = \Pr(p_i^{(k)} \leq t) = (1 - \pi_k)t + \pi_k G_k(t)$ ,  $t \in$   
 704  $[0, 1]$ , where  $0 \leq \pi_k \leq 1$  and  $G_k$  is continuous. Let  $R_k$  denote the number of rejections from applying  
 705 the BH procedure at level  $\alpha$  to method  $k$ , and define the rejection proportion  $r_{k,n} := \frac{R_k}{n}$ . Then there  
 706 exists a constant  $r_k \in [0, 1]$ , such that,  $r_{k,n} \xrightarrow{\text{a.s.}} r_k \quad (n \rightarrow \infty)$ .*

708 **Lemma 2** (Convergence of BH-based weights). *Consider  $K$  detection methods, each with score  
 709 function  $S^{(1)}, \dots, S^{(K)}$ . For each method  $k$ , let p-values on the total dataset  $\mathcal{D}_{\text{total}}$  be  $\{p_i^{(k)}\}_{i=1}^n$ .  
 710 Apply the BH procedure at level  $\alpha$  separately to each method, producing the rejection threshold  $t_{\text{BH}}^{(k)}$   
 711 and the number of rejections  $R_k = |\{Z_i \in \mathcal{D}_{\text{total}} : p_i^{(k)} \leq t_{\text{BH}}^{(k)}\}|$ . Define the normalized data-driven  
 712 weights  $w_k = \frac{R_k}{\sum_{j=1}^K R_j}$ . Then, there exist deterministic constants  $(w_1^*, \dots, w_K^*)$  with  $\sum_{k=1}^K w_k^* = 1$   
 713 such that  $w_k \xrightarrow{\text{a.s.}} w_k^* \quad \text{for each } k = 1, \dots, K$ .*

716 *Proof.* First, by Lemma BH-limit lemma, for each method  $k$  there exists a deterministic constant  
 717  $r_k \in [0, 1]$  such that the rejection proportion  
 718

$$r_{k,n} := \frac{R_k}{n} \xrightarrow{\text{a.s.}} r_k.$$

721 Since  $K$  is finite, the vector of rejection proportions  $\mathbf{r}_n = (r_{1,n}, \dots, r_{K,n})$  converges almost surely  
 722 to  $\mathbf{r} = (r_1, \dots, r_K)$ .

723 Then, due to  $\sum_{k=1}^K r_k > 0$ , we define the limiting weights  
 724

$$w_k^* := \frac{r_k}{\sum_{j=1}^K r_j}, \quad k = 1, \dots, K.$$

725 The sum of the sample proportions  $\sum_{k=1}^K r_{k,n}$  is eventually positive almost surely, so the weights  $w_k$   
 726 are well-defined for large  $n$ .

727 Finally, consider the continuous mapping  
 728

$$h : \{x \in \mathbb{R}^K : \sum_i x_i \neq 0\} \rightarrow \mathbb{R}^K, \quad h(x) = \left( \frac{x_1}{\sum_i x_i}, \dots, \frac{x_K}{\sum_i x_i} \right),$$

729 which maps the rejection proportions to the weights. Applying the continuous mapping theorem to  
 730 the almost-sure convergence of  $\mathbf{r}_n$  gives

$$h(\mathbf{r}_n) = (w_1, \dots, w_K) \xrightarrow{\text{a.s.}} h(\mathbf{r}) = (w_1^*, \dots, w_K^*),$$

731 establishing the almost-sure convergence of the data-driven weights. Convergence in probability  
 732 follows immediately.  $\square$

733 Base on Lemma 2, we can give the following lemma.

734 **Lemma 3.** *Let  $p_i^{(1)}, \dots, p_i^{(K)}$  be the p-values corresponding to a given sample  $i$ , each satisfying  
 735  $p_i^{(k)} \sim \text{Uniform}[0, 1]$  under the null hypothesis  $H_0$ . We have, the aggregated p-value  $p_i^{\text{agg}}$  is  
 736 uniformly distributed on  $[0, 1]$  under  $H_0$ . $W$*

737 *Proof.* In this proof, we first consider the case where the weights are fixed, and then extend the result  
 738 to the setting with data-driven weights. For simplicity, the fixed weights are denoted as  $w_k^*$  for each  
 739 candidate  $k = 1, \dots, K$ .

740 Let  $U_k = p_i^{(k)} \sim \text{Uniform}[0, 1]$ . Define the transformed variable  
 741

$$X_k = \tan[\pi(0.5 - U_k)].$$

742 Now we prove that  $X_k \sim \text{Cauchy}(0, 1)$ . To see this, recall that the cumulative distribution function  
 743 (CDF) of the standard Cauchy distribution is  
 744

$$F(x) = \frac{1}{2} + \frac{1}{\pi} \arctan(x),$$

756 whose inverse is

$$757 \quad F^{-1}(u) = \tan [\pi(u - 0.5)].$$

758 Therefore, if  $U_k \sim \text{Uniform}[0, 1]$ , then,

$$759 \quad X_k = \tan [\pi(0.5 - U_k)] = -\tan [\pi(U_k - 0.5)] \sim \text{Cauchy}(0, 1),$$

760 since the Cauchy distribution is symmetric about zero.

761 Now, consider the weighted sum,

$$762 \quad T^* = \sum_{k=1}^K w_k^* X_k.$$

763 Because the Cauchy distribution is stable under linear combinations Feller (1991), we have,

$$764 \quad T^* \sim \text{Cauchy}(0, 1).$$

765 Finally, we apply the inverse CDF of the standard Cauchy distribution to obtain the aggregated  
766 p-value,

$$767 \quad p_i^{*,\text{agg}} = 1 - F(T_i^*) = \frac{1}{2} - \frac{1}{\pi} \arctan(T_i^*).$$

768 The distribution of  $p_i^{*,\text{agg}}$  can be directly verified by Liu & Xie (2020) as a uniform distribution.

769 Next, we consider aggregated p-values based on data-driven weights. It suffices to prove the  
770 convergence between  $T$  and  $T^*$ . Denote

$$771 \quad \Delta_k = w_k - w_k^*.$$

772 Then,

$$773 \quad T - T^* = \sum_{k=1}^K (w_k - w_k^*) X_k = \sum_{k=1}^K \Delta_k X_k \leq \sum_{k=1}^K |\Delta_k| |X_k|.$$

774 Fix any  $k$ . Since  $X_k$  is standard Cauchy and  $\Delta_k = o_p(1)$ , note the linear scaling property of Cauchy  
775 distributions,

$$776 \quad \Delta_k X_k \sim \text{Cauchy}(0, |\Delta_k|).$$

777 As  $|\Delta_k| \rightarrow 0$  in probability, the scale parameter of  $\Delta_k X_k$  converges to zero. By the definition of  
778 convergence in distribution, this implies

$$779 \quad \Delta_k X_k \xrightarrow{p} 0,$$

780 i.e., each term is  $o_p(1)$ .

781 Since  $K$  is fixed, a finite sum of  $o_p(1)$  terms is still  $o_p(1)$ ,

$$782 \quad \sum_{k=1}^K \Delta_k X_k = o_p(1).$$

783 Thus,

$$784 \quad T - T^* = o_p(1).$$

785 Since  $T^*$  is a finite linear combination of independent standard Cauchy random variables, it is also  
786 Cauchy,

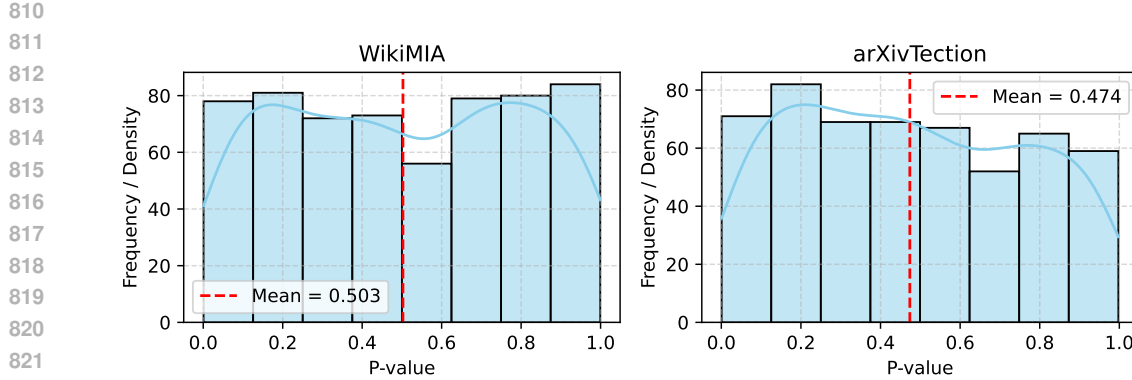
$$787 \quad T^* = \sum_{k=1}^K w_k X_k \sim \text{Cauchy}\left(0, \sum_{k=1}^K |w_k|\right).$$

788 By Slutsky's theorem, adding a term that is  $o_p(1)$  does not change the limiting distribution. Therefore,

$$789 \quad T = T^* + o_p(1) \implies T \xrightarrow{d} T^*.$$

800 This completes the proof. □

801 After establishing the theoretical foundation, we empirically examine the distribution of the aggregated  
802 p-values,  $p_i^{\text{agg}}$ . Specifically, we extract  $p_i^{\text{agg}}$  from two benchmark datasets, WikiMIA and  
803 arXivTection, and visualize their empirical distributions, as shown in Figure 6. The results indicate  
804 that the aggregated p-values approximately follow a uniform distribution, which provides empirical  
805 support for the validity of Lemma 3.

Figure 6: The p-value distribution of  $p_i^{\text{agg}}$  on datasets WikiMIA and arXivTection.

## 10 APPENDIX B

In this section, we theoretically demonstrate that TD4Eval achieves asymptotic optimality in controlling the FDR while maintaining high statistical power, as established in Theorems 1 and 2.

**Theorem 1** (FDR Control of TD4Eval). *Suppose we are given a set of training data detection methods, each associated with a score function  $S^{(1)}, \dots, S^{(K)}$ . Let the corresponding p-values be defined as  $\{p_j^{(1)}\}_{j \in [n]}, \dots, \{p_j^{(K)}\}_{j \in [n]}$ , where each p-value is computed as  $p_i^{(k)} = \mathbb{P}_{S \sim \mathcal{S}_{\text{ref}}^{(k)}}(S \leq S_i^{(k)})$ . Then, the TD4Eval procedure controls the FDR at level  $\alpha$ , i.e.,*

$$\text{FDR} := \mathbb{E} \left[ \frac{|\hat{\mathcal{S}} \cap \mathcal{D}_{\text{con}}|}{|\hat{\mathcal{S}}| \vee 1} \right] \leq \alpha. \quad (14)$$

*Proof.* From Lemma 3, the aggregated p-value  $p_i^{\text{agg}}$ , computed from  $p_i^{(1)}, \dots, p_i^{(K)}$ , is approximately uniformly distributed on  $[0, 1]$  under  $H_0$ . This satisfies the assumptions required by the BH procedure: namely, that p-values under  $H_0$  are uniformly distributed.

According to the BH procedure Benjamini & Hochberg (1995); Benjamini & Yekutieli (2001), if the p-values under the null hypothesis  $H_0$  are independent and uniformly distributed, then the BH procedure guarantees control of the FDR at the nominal level  $\alpha$ . Furthermore, Theorem 4 in Storey et al. (2004) relaxes the independence assumption required by the BH procedure, providing theoretical guarantees for FDR control under the dependence of p-values. Since the aggregated p-values used in TD4Eval approximately satisfy the required assumptions, applying the BH procedure ensures that the FDR is controlled at the desired level. Therefore, the TD4Eval procedure controls the FDR at level  $\alpha$ , as claimed. i.e.,

$$\text{FDR} := \mathbb{E} \left[ \frac{|\hat{\mathcal{S}} \cap \mathcal{D}_{\text{con}}|}{|\hat{\mathcal{S}}| \vee 1} \right] \leq \alpha.$$

□

Before giving the theorem 2, we introduce the following lemmas, which are useful for proving the power consistency.

**Lemma 4** (Theorem 6 in Storey et al. (2004), finite sample version). *Fix  $t \in (0, 1]$  and let  $q \in (0, 1)$ . Then for any  $\epsilon > 0$ ,*

$$\mathbb{P} \left( \left| \widehat{\text{FDR}}(t) - \text{FDR}(t) \right| > \epsilon \right) \leq 2 \exp \left( -2n \cdot \frac{\pi_0^2 t^2 \epsilon^2}{\text{FDR}(t)^4} \right).$$

This follows from applying Hoeffding's inequality to  $\widehat{G}_n(t)$  and noting that  $x \mapsto \pi_0 t / x$  is Lipschitz on bounded away-from-zero intervals.

Define the ideal threshold,

$$t^* := \sup \{t \in (0, 1] : \text{FDR}(t) \leq \alpha\},$$

864 and the empirical threshold (e.g. Benjamini-Hochberg with plug-in  $\pi_0$ ),  
 865

$$866 t_{BH} := \sup\{t \in (0, 1] : \widehat{\text{FDR}}(t) \leq \alpha\}.$$

867 We now state a finite-sample deviation bound for  $|t_{BH} - t^*|$ .  
 868

869 **Lemma 5** (Finite-Sample Deviation of BH Threshold). *Suppose  $\text{FDR}(t)$  is strictly increasing and  
 870 continuously differentiable in a neighborhood  $[t^* - \epsilon, t^* + \epsilon]$ , and its derivative satisfies  $\text{FDR}'(t) \geq  
 871 \alpha > 0$  in that region. Then for any  $\epsilon > 0$  such that  $t^* - \epsilon > 0$ , we have,*

$$872 \mathbb{P}(t_{BH} < t^* - \epsilon) \leq 2 \exp\left(-2n \cdot \frac{\pi_0^2(t^* - \epsilon)^2 \epsilon^2}{\alpha^2}\right),$$

$$873 \mathbb{P}(t_{BH} > t^* + \epsilon) \leq 2 \exp\left(-2n \cdot \frac{\pi_0^2(t^* + \epsilon)^2 \epsilon^2}{\alpha^4}\right).$$

877 *Proof.* We analyze the lower tail; the upper bound follows similarly.  
 878

879 Suppose  $t_{BH} < t^* - \epsilon$ , i.e., there is no  $t \in [t^* - \epsilon, t^*]$  such that  $\widehat{\text{FDR}}(t) \leq \alpha$ . Since  $\text{FDR}(t) \leq \alpha$   
 880 on  $[0, t^*]$ , we must have,  
 881

$$882 \widehat{\text{FDR}}(t) > \alpha \geq \text{FDR}(t), \quad \forall t \in [t^* - \epsilon, t^*].$$

883 In particular, for  $t = t^* - \epsilon$ ,  
 884

$$885 \widehat{\text{FDR}}(t) - \text{FDR}(t) > \alpha - \text{FDR}(t) \geq \alpha\epsilon,$$

886 where the last inequality comes from the first-order Taylor expansion,  
 887

$$888 \text{FDR}(t^*) - \text{FDR}(t^* - \epsilon) \geq \alpha\epsilon.$$

889 Therefore,

$$890 \mathbb{P}(t_{BH} < t^* - \epsilon) \leq \mathbb{P}\left(\widehat{\text{FDR}}(t^* - \epsilon) - \text{FDR}(t^* - \epsilon) > \alpha\epsilon\right),$$

892 which is bounded by Lemma 4,

$$893 \leq 2 \exp\left(-2n \cdot \frac{\pi_0^2(t^* - \epsilon)^2(\alpha\epsilon)^2}{\text{FDR}(t^* - \epsilon)^4}\right) \leq 2 \exp\left(-2n \cdot \frac{\pi_0^2(t^* - \epsilon)^2\epsilon^2}{\alpha^2}\right).$$

895  $\square$

897 **Theorem 2** (Asymptotic Power Consistency of TD4Eval). *Assume that for each  $k \in [K]$  and  
 898  $Z_j \in \mathcal{D}_{\text{clean}}$ ,  $\Pr(p_j^{(k)} \leq c) \geq 1 - \delta$  where  $\delta = o(\sqrt{\log n/n})$  and  $c$  is a constant, and the density  
 899 function of  $p_j^{\text{agg}}$  for  $Z_j \in \mathcal{D}_{\text{clean}}$  has an upper bound  $C_f > 0$ , we have,*  
 900

$$901 \text{Power} := \mathbb{E}\left[\frac{|\hat{\mathcal{S}} \cap \mathcal{D}_{\text{clean}}|}{|\mathcal{D}_{\text{clean}}| \vee 1}\right] \geq 1 - C\sqrt{\log n/n}.$$

905 *Proof.* By Lemma 3, the aggregated p-value  $p_i^{\text{agg}}$ , computed from  $p_i^{(1)}, \dots, p_i^{(K)}$ , is uniformly  
 906 distributed on  $[0, 1]$  under  $H_0$ . So  $p_1^{\text{agg}}, \dots, p_n^{\text{agg}}$  are drawn from the two-group mixture model,  
 907

$$908 p_i^{\text{agg}} \sim \pi_0 \cdot U[0, 1] + \pi_1 \cdot F_1, \quad \text{where } \pi_0 + \pi_1 = 1,$$

909 with  $F_1$  being a continuous distribution supported on  $[0, 1]$ .  
 910

911 Define the empirical CDF,  
 912

$$913 \hat{G}_n(t) := \frac{1}{n} \sum_{i=1}^n \mathbf{1}\{p_i^{\text{agg}} \leq t\}, \quad G(t) := \pi_0 t + \pi_1 F_1(t).$$

915 The true and estimated FDR curves are defined respectively as,  
 916

$$917 \text{FDR}(t) := \frac{\pi_0 t}{G(t)}, \quad \widehat{\text{FDR}}(t) := \frac{\pi_0 t}{\hat{G}_n(t)}.$$

918 Define the ideal threshold,

$$919 \quad t^* := \sup\{t \in (0, 1] : \text{FDR}(t) \leq \alpha\},$$

920 and the empirical threshold (e.g. Benjamini-Hochberg with plug-in  $\pi_0$ ),

$$921 \quad t_{BH} := \sup\{t \in (0, 1] : \widehat{\text{FDR}}(t) \leq \alpha\}.$$

922 By the definition of power, we have,

$$923 \quad \text{Power} := \frac{1}{|\mathcal{D}_{\text{clean}}|} \sum_{Z_i \in \mathcal{D}_{\text{clean}}} \mathbb{P}(p_i^{agg} \leq t_{BH}) = \Pr_{p_i^{agg} \sim F_1}(p_i^{agg} \leq t_{BH}).$$

924 Applying Lemma 5, we know that at probability  $2 \exp\left(-2n \cdot \frac{\pi_0^2(t^* - \epsilon)^2 \epsilon^2}{\alpha^2}\right)$ ,  $t_{BH} < t^* - \epsilon$  for any  $\epsilon > 0$ .

925 Then it has,

$$\begin{aligned} 926 \quad \Pr_{p_i^{agg} \sim F_1}(p_i^{agg} \leq t_{BH}) &= 1 - \Pr_{p_i^{agg} \sim F_1}(p_i^{agg} > t_{BH}) \\ 927 &= 1 - \Pr_{p_i^{agg} \sim F_1}(p_i^{agg} > t_{BH}, t_{BH} < t^* - \epsilon) - \Pr_{p_i^{agg} \sim F_1}(p_i^{agg} > t_{BH}, t_{BH} \geq t^* - \epsilon) \\ 928 &\geq 1 - \Pr_{p_i^{agg} \sim F_1}(p_i^{agg} > t^* - \epsilon, t_{BH} \geq t^* - \epsilon) - \Pr_{p_i^{agg} \sim F_1}(p_i^{agg} > t_{BH}, t_{BH} < t^* - \epsilon) \\ 929 &\geq \Pr_{p_i^{agg} \sim F_1}(p_i^{agg} \leq t^* - \epsilon) - \Pr_{p_i^{agg} \sim F_1}(t_{BH} < t^* - \epsilon) \\ 930 &\geq F_1(t^* - \epsilon) - 2 \exp\left(-2n \cdot \frac{\pi_0^2(t^* - \epsilon)^2 \epsilon^2}{\alpha^2}\right). \end{aligned}$$

931 Moreover, under the assumptions in Theorem 2, by the definition of the weight where  $\sum_{i=k}^K w_k = 1$ ,  
932 there exists  $\ell \in [K]$  such that  $\sum_{k=1}^K w_k \tan[(0.5 - p_i^{(k)})\pi] \geq \tan[(0.5 - p_i^{(\ell)})\pi]$ . Then we have,

$$\begin{aligned} 933 \quad F_1(t^*) &= \Pr(p_i^{agg} \leq t^*) = \Pr\left(\sum_{k=1}^K w_k \tan[(0.5 - p_i^{(k)})\pi] \geq \tan[(0.5 - t^*)\pi]\right) \\ 934 &\geq \Pr\left(\tan[(0.5 - p_i^{(\ell)})\pi] \geq \tan[(0.5 - t^*)\pi]\right) \\ 935 &\geq \Pr\left(\tan[(0.5 - p_i^{(\ell)})\pi] \geq \tan[(0.5 - t^*)\pi] \mid p_i^{(\ell)} < 0.5\right) \Pr(p_i^{(\ell)} < 0.5) \end{aligned}$$

936 If  $t^* \leq 0.5$ , as the function,  $x \mapsto \tan[(0.5 - x)\pi]$  is strictly decreasing on  $[0, 0.5)$ , we have  
937  $p_i^{(\ell)} \leq t^*$  is equivalent to,

$$938 \quad \tan[(0.5 - p_i^{(\ell)})\pi] \geq \tan[(0.5 - t^*)\pi].$$

939 Therefore,

$$940 \quad \Pr\left(\tan[(0.5 - p_i^{(\ell)})\pi] \geq \tan[(0.5 - t^*)\pi] \mid p_i^{(\ell)} < 0.5\right) \Pr(p_i^{(\ell)} < 0.5) = \Pr(p_i^{(\ell)} \leq \min(t^*, 0.5)) \geq 1 - \delta.$$

941 Otherwise, if  $t^* > 0.5$ , we have  $\Pr\left(\tan[(0.5 - p_i^{(\ell)})\pi] \geq \tan[(0.5 - t^*)\pi] \mid p_i^{(\ell)} < 0.5\right) = 1$ . This  
942 leads to,

$$943 \quad \Pr\left(\tan[(0.5 - p_i^{(\ell)})\pi] \geq \tan[(0.5 - t^*)\pi] \mid p_i^{(\ell)} < 0.5\right) \Pr(p_i^{(\ell)} < 0.5) \geq \Pr(p_i^{(\ell)} < c) \geq 1 - \delta.$$

944 Combining together, we have,

$$945 \quad F_1(t^*) \geq 1 - \delta.$$

946 Then note that  $F_1(t^* - \epsilon) \geq F_1(t^*) - f_1(t^*)\epsilon$ . By the condition of  $F_1(t^*) = 1 - \delta$  and  $f_1(t) \leq C$ ,  
947 we have  $F_1(t^* - \epsilon) \geq 1 - C\epsilon$ . Putting together and taking  $\epsilon = \frac{\pi_0 t^*}{\alpha} \sqrt{\log n / (2n)}$ , we have,

$$\begin{aligned} 948 \quad \text{Power} &\geq 1 - \delta - C_f \epsilon - 2 \exp\left(-2n \cdot \frac{\pi_0^2(t^* - \epsilon)^2 \epsilon^2}{\alpha^2}\right) \\ 949 &= 1 - \delta - C_f \frac{\pi_0 t^*}{\alpha} \sqrt{\frac{\log n}{2n}} - \frac{2}{n}, \end{aligned}$$

972 Since  $\frac{2}{n} = o\left(\sqrt{\frac{\log n}{n}}\right)$  and all fixed factors can be absorbed into a universal constant, the bound  
 973 simplifies to  $1 - C\sqrt{\frac{\log n}{n}}$ , where  $C > 0$  is a constant depending on the testing level, the null  
 974 proportion, and certain distributional characteristics.  $\square$   
 975  
 976

## 977 11 APPENDIX C

### 978 11.1 BASELINES

979 We provide detailed descriptions of the baseline methods used in our experiments:  
 980

- 981 • **PPL** Li (2023): This method uses the perplexity of a target model on a given input to infer  
 982 whether the input was part of the training data. Lower perplexity often indicates higher  
 983 likelihood of memorization.
- 984 • **Lowercase** Carlini et al. (2021): This method calibrates the model’s likelihood by comparing  
 985 the perplexity of the original text with that of its lowercased version.
- 986 • **Zlib** Carlini et al. (2021): This method uses compression entropy as a reference to calibrate  
 987 the model’s likelihood. The idea is that memorized or redundant content tends to be more  
 988 compressible, and thus this ratio can help distinguish training data from non-training data.
- 989 • **Grad** Hu et al.: A gradient-based method that computes the norm of the gradient of the loss  
 990 with respect to model parameters. Smaller gradient norms are often associated with training  
 991 data.
- 992 • **Min-K%** Shi et al.: This method computes the average log-likelihood of the lowest  $K\%$   
 993 tokens in a sequence. The  $K$  is set to 20.
- 994 • **Min-K%++** Zhang et al. (2024b): An improved version of Min-K% that incorporates  
 995 token-level calibration to enhance detection accuracy. The  $K$  is set to 20.

996 Moreover, to evaluate the effectiveness of our adaptive weighting strategy, we introduce three  
 997 TD4Eval variants: BH-Average, BH-Random, and BH-Max.  
 998

- 1001 • **BH-Average**: discards the learned weights and instead averages the p-values uniformly.
- 1002 • **BH-Max**: selects the best-performing detection method for each instance without fusion.
- 1003 • **BH-Random**: assigns random weights to the detection methods.

### 1004 11.2 DATASETS

1005 We evaluate our method on three benchmark datasets commonly used in training data detection:  
 1006 **WikiMIA** Shi et al., **ArXivTection** Duarte et al. (2024), **BBC Real Time** Li et al. (2024), and  
 1007 **MIMIR** Duan et al.. These datasets contain both training data and non-training data, and are  
 1008 constructed to reflect realistic overlaps with pre-training corpora of large language models. Below,  
 1009 we briefly describe each dataset:  
 1010

- 1011 • **WikiMIA** Shi et al.: Contains Wikipedia event texts, where membership is determined  
 1012 based on publication timestamps. Events occurring before 2017 are treated as contaminated  
 1013 data, while those after 2023 are considered clean data.
- 1014 • **ArXivTection** Duarte et al. (2024): A benchmark dataset constructed from 50 research  
 1015 papers on arXiv, designed to evaluate pretraining data detection in scientific domains. Papers  
 1016 published before 2022 are labeled as contaminated data, while those from 2023 are labeled  
 1017 as clean data.
- 1018 • **BBC Real Time** Li et al. (2024): Comprises BBC news articles published between January  
 1019 2017 and August 2024. Following the setup in Shi et al., articles from 2017 are used as  
 1020 contaminated data, while those from 2024 serve as clean data.
- 1021 • **MIMIR** Duan et al.: Constructed from the Pile dataset Gao et al. (2020), where training  
 1022 samples are drawn from the train split and non-training samples from the test split. In our  
 1023 experiments, we select seven representative subsets—*DM Mathematics*, *GitHub*, *Pile CC*,  
 1024 *PubMed Central*, *ArXiv*, *HackerNews*, and *Wikipedia*—and report the averaged results.  
 1025

1026

1027

Table 3: Statistics of the evaluation datasets used in our experiments.

1028

1029

| Dataset       | Type           | Contaminated Data | Clean Data | Total |
|---------------|----------------|-------------------|------------|-------|
| WikiMIA       | Validation Set | 258               | 237        | 495   |
|               | Test Set       | 603               | 552        | 1155  |
| ArXivTection  | Validation Set | 228               | 236        | 464   |
|               | Test Set       | 534               | 550        | 1084  |
| BBC Real Time | Validation Set | 983               | 1003       | 1986  |
|               | Test Set       | 2293              | 2343       | 4636  |
| MIMIR         | Validation Set | 1050              | 1050       | 2100  |
|               | Test Set       | 2450              | 2450       | 4900  |

1038

1039

Table 4: The detection performance of OPT-6.7B on three datasets. FDR (lower is better), Power (higher is better), ACC (higher is better), AUC (higher is better). Bold indicates the best result per model. For TD4Eval, we report the mean and standard deviation across ten independent runs.

1040

1041

| Method    | WikiMIA      |              |              |              | arXivTection |              |              |              | BBC Real Time |              |              |              |
|-----------|--------------|--------------|--------------|--------------|--------------|--------------|--------------|--------------|---------------|--------------|--------------|--------------|
|           | FDR ↓        | Power ↑      | ACC ↑        | AUC ↑        | FDR ↓        | Power ↑      | ACC ↑        | AUC ↑        | FDR ↓         | Power ↑      | ACC ↑        | AUC ↑        |
| PPL       | 0.168        | 0.821        | 0.835        | 0.923        | 0.156        | 0.839        | 0.839        | 0.915        | 0.192         | 0.604        | 0.727        | 0.808        |
| Lowercase | 0.208        | 0.671        | 0.758        | 0.858        | 0.212        | 0.588        | 0.710        | 0.816        | 0.190         | <b>0.617</b> | <b>0.733</b> | 0.813        |
| Zlib      | 0.244        | 0.545        | 0.698        | 0.785        | 0.243        | 0.449        | 0.646        | 0.757        | 0.292         | 0.356        | 0.600        | 0.707        |
| Grad      | 0.190        | 0.717        | 0.784        | 0.868        | 0.167        | 0.732        | 0.789        | 0.873        | 0.205         | 0.586        | 0.714        | 0.803        |
| Min-K%    | 0.167        | 0.895        | 0.864        | 0.936        | 0.136        | <b>0.898</b> | 0.877        | 0.948        | 0.221         | 0.513        | 0.680        | 0.773        |
| Min-K++   | 0.153        | <b>0.974</b> | 0.903        | 0.972        | 0.154        | 0.812        | 0.829        | 0.906        | 0.202         | 0.595        | 0.719        | 0.807        |
| TD4Eval   | <b>0.100</b> | 0.964        | <b>0.931</b> | <b>0.979</b> | <b>0.083</b> | 0.849        | <b>0.884</b> | <b>0.953</b> | <b>0.098</b>  | 0.506        | 0.722        | <b>0.856</b> |
| (std)     | ±0.017       | ±0.012       | ±0.006       | ±0.003       | ±0.021       | ±0.030       | ±0.006       | ±0.004       | ±0.006        | ±0.037       | ±0.016       | ±0.004       |

1053

1054

For each dataset, we randomly select 30% as a validation set and use the remaining 70% for testing. The validation set is used to select decision thresholds or estimate the distribution of training data, while the test set is reserved for final evaluation. Detailed dataset statistics are provided in Table 3.

1055

1056

### 11.3 IMPLEMENTATION DETAILS

1057

1058

In real-world contamination detection, we require a threshold  $t$  to determine whether a data point is contaminated. To obtain this threshold, following the settings in Shi et al.; Hu et al.; Zhang et al. (2024a), we randomly select 30% of the dataset as a validation set, while the remaining 70% is used as the test set. The optimal classification threshold is determined by maximizing detection accuracy on the validation set. In addition, our method requires access to a subset of known contaminated samples in order to estimate the p-values. Following a similar setting as in Zhang et al. (2024a), we use the contaminated samples from the validation set for this purpose. For the baseline configurations, we follow the settings from their original papers. Specifically, the parameter K in both Min-K and Min-K++ is set to 20. Except for the *Effect of  $\alpha$*  experiment, the value of  $\alpha$  is fixed at 0.15 in all other settings. Furthermore, as our approach relies on integrating various training data detection methods, we incorporate all baseline methods for a comprehensive evaluation. All experiments are conducted on two NVIDIA A100 GPUs (40GB each) and a 16-core Intel Xeon Gold 6426Y CPU. All implementations are based on PyTorch.

1072

1073

### 11.4 MAIN RESULTS

1074

1075

The results for OPT-6.7B and MIMIR are provided in the Tables 4 and 5, which shows the same result of main paper. Specifically,

1076

1077

- *Finding 1 – TD4Eval achieves the lowest FDR across all datasets and model settings, demonstrating its strong ability to suppress false positives.* Compared to the strongest baseline, TD4Eval achieves the best FDR result, indicating a substantial improvement in precision when identifying clean data.

1080

1081 Table 5: Results on the challenging MIMIR benchmark with Pythia-2.8B

| Method         | DM Mathematics |              |              |              | GitHub       |              |              |              | Pile CC      |              |              |              | PubMed Central |              |              |              |
|----------------|----------------|--------------|--------------|--------------|--------------|--------------|--------------|--------------|--------------|--------------|--------------|--------------|----------------|--------------|--------------|--------------|
|                | FDR↓           | Power↑       | ACC↑         | AUC↑         | FDR↓         | Power↑       | ACC↑         | AUC↑         | FDR↓         | Power↑       | ACC↑         | AUC↑         | FDR↓           | Power↑       | ACC↑         | AUC↑         |
| PPL            | 0.380          | 0.489        | 0.594        | 0.647        | 0.316        | 0.303        | 0.581        | 0.669        | 0.235        | 0.549        | 0.690        | 0.771        | 0.319          | 0.414        | 0.610        | 0.688        |
| Lowercase      | 0.425          | 0.317        | 0.541        | 0.642        | 0.270        | 0.317        | 0.600        | 0.687        | 0.234        | 0.654        | 0.727        | 0.794        | 0.323          | 0.497        | 0.630        | 0.695        |
| Zlib           | 0.348          | 0.509        | 0.619        | 0.649        | 0.311        | 0.323        | 0.589        | 0.671        | 0.320        | 0.491        | 0.630        | 0.717        | 0.343          | 0.406        | 0.597        | 0.674        |
| Grad           | 0.196          | <b>0.963</b> | 0.864        | <b>0.975</b> | 0.201        | <b>0.820</b> | 0.807        | 0.875        | 0.194        | <b>0.880</b> | 0.834        | 0.897        | 0.239          | <b>0.711</b> | 0.744        | 0.821        |
| Min-K%         | 0.351          | 0.497        | 0.614        | 0.663        | 0.225        | 0.403        | 0.643        | 0.724        | 0.209        | 0.563        | 0.707        | 0.803        | 0.295          | 0.471        | 0.637        | 0.721        |
| Min-K%++       | 0.161          | 0.880        | 0.856        | 0.934        | 0.142        | 0.809        | 0.837        | <b>0.928</b> | 0.188        | 0.777        | 0.799        | 0.888        | 0.238          | 0.703        | 0.741        | <b>0.875</b> |
| <b>TD4Eval</b> | <b>0.145</b>   | <b>0.963</b> | <b>0.900</b> | 0.974        | <b>0.072</b> | 0.740        | <b>0.841</b> | <b>0.928</b> | <b>0.177</b> | 0.863        | <b>0.839</b> | <b>0.911</b> | <b>0.101</b>   | 0.611        | <b>0.771</b> | 0.868        |
| Method         | ArXiv          |              |              |              | HackerNews   |              |              |              | WikiMedia    |              |              |              | Average        |              |              |              |
|                | FDR↓           | Power↑       | ACC↑         | AUC↑         | FDR↓         | Power↑       | ACC↑         | AUC↑         | FDR↓         | Power↑       | ACC↑         | AUC↑         | FDR↓           | Power↑       | ACC↑         | AUC↑         |
| PPL            | 0.321          | 0.363        | 0.596        | 0.676        | 0.362        | 0.594        | 0.629        | 0.702        | 0.318        | 0.509        | 0.636        | 0.685        | 0.321          | 0.475        | 0.624        | 0.691        |
| Lowercase      | 0.380          | 0.326        | 0.563        | 0.652        | 0.371        | 0.600        | 0.623        | 0.706        | 0.323        | 0.497        | 0.630        | 0.677        | 0.332          | 0.487        | 0.616        | 0.683        |
| Zlib           | 0.390          | 0.300        | 0.554        | 0.653        | 0.371        | 0.509        | 0.604        | 0.624        | 0.316        | 0.537        | 0.644        | 0.707        | 0.343          | 0.439        | 0.606        | 0.669        |
| Grad           | 0.197          | 0.806        | 0.804        | 0.881        | 0.292        | <b>0.874</b> | 0.757        | 0.826        | 0.255        | 0.877        | 0.789        | <b>0.882</b> | 0.225          | 0.847        | 0.800        | 0.894        |
| Min-K%         | 0.269          | 0.466        | 0.647        | 0.718        | 0.302        | 0.700        | 0.699        | 0.761        | 0.272        | 0.520        | 0.663        | 0.733        | 0.274          | 0.550        | 0.660        | 0.732        |
| Min-K%++       | 0.202          | 0.769        | 0.787        | 0.850        | 0.286        | 0.700        | 0.710        | 0.866        | 0.273        | 0.783        | 0.744        | 0.841        | 0.213          | 0.774        | 0.782        | 0.878        |
| <b>TD4Eval</b> | <b>0.146</b>   | <b>0.812</b> | <b>0.836</b> | <b>0.883</b> | <b>0.158</b> | 0.669        | <b>0.771</b> | <b>0.877</b> | <b>0.117</b> | <b>0.879</b> | <b>0.880</b> | 0.881        | <b>0.131</b>   | <b>0.802</b> | <b>0.834</b> | <b>0.896</b> |

1100 • *Finding 2 – TD4Eval maintains competitive or superior detection power in most settings.* It achieves  
 1101 near-perfect power on two datasets and performs robustly on the third, showing that it can effectively  
 1102 recall clean samples while maintaining low FDR.

1103 • *Finding 3 – TD4Eval consistently achieves the highest overall accuracy across different datasets  
 1104 and models.* This reflects its comprehensive effectiveness in both minimizing false detections and  
 1105 correctly identifying clean data, which is crucial for downstream applications.

1106 Overall, our proposed method TD4Eval consistently outperforms existing baselines across all evalua-  
 1107 tion metrics, demonstrating its robustness and effectiveness in mitigating the impact of contaminated  
 1108 data to support reliable model evaluation.

## 1110 12 APPENDIX D

### 1111 12.1 LLM EVALUATION BENCHMARK

1112 We evaluate our method on four widely used large language model (LLM) evaluation benchmarks:  
 1113 SimpleQA Wei et al. (2024), GPQA Rein et al. (2023), TruthfulQA Lin et al. (2022), and ARC-  
 1114 C Clark et al. (2018). These datasets are designed to measure complementary aspects of LLM. Below,  
 1115 we briefly describe each benchmark:

- 1116 • **SimpleQA** Wei et al. (2024): A benchmark designed to evaluate models on straightforward  
 1117 factual question answering. The dataset emphasizes clarity and unambiguous answers,  
 1118 making it suitable for measuring baseline factual knowledge.
- 1119 • **GPQA** Rein et al. (2023): A graduate-level benchmark focusing on expert-level knowledge  
 1120 across diverse scientific domains. Questions require precise reasoning and domain expertise,  
 1121 providing a challenging test for LLMs beyond basic factual recall.
- 1122 • **TruthfulQA** Lin et al. (2022): Consists of questions crafted to expose common misconcep-  
 1123 tions or false associations that language models may generate. The benchmark evaluates a  
 1124 model’s ability to provide factually correct responses while resisting the tendency to produce  
 1125 plausible but false statements.
- 1126 • **ARC-C** Clark et al. (2018): The “Challenge” subset of the AI2 Reasoning Challenge  
 1127 benchmark. It is composed of grade-school science exam questions requiring reasoning,  
 1128 inference, and integration of knowledge.

1129 For each dataset, we follow the standard evaluation setup proposed in the corresponding papers.

1134  
 1135 Table 6: Examples of question-answer pairs from different datasets and their corresponding prompt  
 1136 format used for fine-tuning.

| 1137 <b>Original QA Pair</b> | 1138 <b>Formatted Prompt for Fine-tuning</b>   |  |
|------------------------------|--|--|
| 1139 <b>SimpleQA</b>         | 1139     ### Question:<br>1140     What is the capital of France?<br>1141     A: Paris.  | 1139     What is the capital of France?<br>1140     ### Answer:<br>1141     Paris.   |
| 1142 <b>GPQA</b>             | 1142     ### Question:<br>1143     Q: You come across an algorithm that gives the<br>1144     following output (written as input -> output):<br>1145     AGG -> 115<br>1146     TGCTGA -> 176<br>1147     What value does ACAGTGACC give?<br>1148     A: 315 | 1142     You come across an algorithm<br>1143     that gives the following output<br>1144     (written as input -> output):<br>1145     AGG -> 115<br>1146     TGCTGA -> 176<br>1147     What value does ACAGTGACC give?<br>1148     ### Answer:<br>1149     315 |
| 1150 <b>TruthfulQA</b>       | 1150     ### Question:<br>1151     Q: What tastes so good that cats ask for it by name?<br>1152     A: Cats can't ask for anything by name.  | 1150     What tastes so good that cats ask<br>1151     for it by name?<br>1152     ### Answer:<br>1153     Cats can't ask for anything by<br>1154     name.  |
| 1155 <b>ARC-C</b>            | 1155     ### Question:<br>1156     Q: What do waves carry through objects?<br>1157     (A) sound (B) light (C) energy (D) water<br>1158     A: (C) energy  | 1155     What do waves carry through<br>1156     objects?<br>1157     (A) sound (B) light (C) energy<br>1158     (D) water<br>1159     ### Answer:<br>1160     (C) energy  |

## 1163 12.2 FINE-TUNING EXPERIMENTAL SETUP

1164 To investigate the practical applicability of TD4Eval in mitigating the impact of test data contamination  
 1165 on model evaluation, we create a controlled synthetic contamination scenario. Specifically, we  
 1166 fine-tune two pre-trained models, **LLaMA-3.1-8B** and **Mistral-7B**, on four evaluation benchmarks:  
 1167 SimpleQA, GPQA, TruthfulQA, and ARC-C. For each dataset, we randomly sample **50%** of its test  
 1168 set and inject it into the fine-tuning data. The fine-tuned models are then re-evaluated on both the full  
 1169 benchmark test sets and the cleaned subsets produced by different contamination detection methods.  
 1170

1171 **Data Preparation.** To simulate evaluation data contamination, we randomly sample half (50%)  
 1172 of each benchmark’s evaluation set and use it as supervised fine-tuning data. Each selected sample  
 1173 is a question-answer (QA) pair, which is formatted into a prompt suitable for instruction tuning.  
 1174 Examples of original QA pairs and their corresponding formatted prompts are shown in Table 6.  
 1175

1176 **Training Configuration.** The fine-tuning is conducted using the Hugging Face transformers and  
 1177 peft libraries. Key hyperparameters are summarized in Table 7.

1179 Table 7: Fine-tuning configuration.

| 1180 <b>LoRA Rank</b> | 1181 <b>LoRA <math>\alpha</math></b> | 1182 <b>Dropout</b> | 1183 <b>Epochs</b> | 1184 <b>Batch Size</b> | 1185 <b>LR</b> | 1186 <b>Scheduler</b> |
|-----------------------|--------------------------------------|---------------------|--------------------|------------------------|----------------|-----------------------|
| 1187 16               | 1188 32                              | 1189 0.1            | 1190 10            | 1191 8                 | 1192 5e-5      | 1193 Cosine           |

## 1184 12.3 RESULTS UNDER DIFFERENT CONTAMINATION LEVELS

1185 In the original paper, we report the results of different data detection methods under contamination.  
 1186 In this section, we evaluate the robustness of different contamination detection methods under 5%,

1188

1189 Table 8: Impact of different detection methods on LLM Evaluation. We simulate a data contamination  
 1190 scenario by fine-tuning LLaMA-3.1-8B on 5% of the SimpleQA training set. Various data detection  
 1191 methods are then employed to retain clean data for LLM evaluation. The effectiveness of a detection  
 1192 method is measured by how closely the resulting model leaderboard aligns with the ground truth  
 1193 ranking, the closer the match, the more effective the method.

| Rank       | SimpleQA<br>(Ground Truth) | SimpleQA<br>(contaminated) | PPL                 | Lowercase           | Zlib                | Grad                | Min-K%              | Min-K%++            | TD4Eval             |
|------------|----------------------------|----------------------------|---------------------|---------------------|---------------------|---------------------|---------------------|---------------------|---------------------|
| 1          | LLaMA-3-70B                | LLaMA-3-70B                | LLaMA-3-70B         | LLaMA-3-70B         | LLaMA-3-70B         | LLaMA-3-70B         | LLaMA-3-70B         | LLaMA-3-70B         | LLaMA-3-70B         |
| 2          | GPT-4o-mini                | GPT-4o-mini                | GPT-4o-mini         | GPT-4o-mini         | GPT-4o-mini         | GPT-4o-mini         | GPT-4o-mini         | GPT-4o-mini         | GPT-4o-mini         |
| 3          | o1-mini                    | o1-mini                    | o1-mini             | o1-mini             | o1-mini             | o1-mini             | o1-mini             | o1-mini             | o1-mini             |
| 4          | Gemini-1.5-Flash           | Gemini-1.5-Flash           | Gemini-1.5-Flash    | Gemini-1.5-Flash    | Gemini-1.5-Flash    | Gemini-1.5-Flash    | Gemini-1.5-Flash    | Gemini-1.5-Flash    | Gemini-1.5-Flash    |
| 5          | Mistral-7B                 | <b>LLaMA-3.1-8B</b>        | <b>LLaMA-3.1-8B</b> | <b>LLaMA-3.1-8B</b> | <b>LLaMA-3.1-8B</b> | <b>LLaMA-3.1-8B</b> | <b>LLaMA-3.1-8B</b> | <b>LLaMA-3.1-8B</b> | Mistral-7B          |
| 6          | Claude-3-Haiku             | Mistral-7B                 | Mistral-7B          | Mistral-7B          | Mistral-7B          | Mistral-7B          | Mistral-7B          | Mistral-7B          | Claude-3-Haiku      |
| 7          | <b>LLaMA-3.1-8B</b>        | Claude-3-Haiku             | Claude-3-Haiku      | Claude-3-Haiku      | Claude-3-Haiku      | Claude-3-Haiku      | Claude-3-Haiku      | Claude-3-Haiku      | <b>LLaMA-3.1-8B</b> |
| 8          | LLaMA-3.2-3B               | LLaMA-3.2-3B               | LLaMA-3.2-3B        | LLaMA-3.2-3B        | LLaMA-3.2-3B        | LLaMA-3.2-3B        | LLaMA-3.2-3B        | LLaMA-3.2-3B        | LLaMA-3.2-3B        |
| <b>FDR</b> | —                          | —                          | 0.050               | 0.050               | 0.050               | 0.050               | 0.050               | 0.050               | <b>0.016</b>        |

1201

1202

1203 Table 9: Impact of different detection methods on LLM Evaluation. We simulate a data contamination  
 1204 scenario by fine-tuning LLaMA-3.1-8B on 10% of the SimpleQA training set. Various data detection  
 1205 methods are then employed to retain clean data for LLM evaluation. The effectiveness of a detection  
 1206 method is measured by how closely the resulting model leaderboard aligns with the ground truth  
 1207 ranking, the closer the match, the more effective the method.

| Rank       | SimpleQA<br>(Ground Truth) | SimpleQA<br>(contaminated) | PPL                 | Lowercase           | Zlib                | Grad                | Min-K%           | Min-K%++            | TD4Eval             |
|------------|----------------------------|----------------------------|---------------------|---------------------|---------------------|---------------------|------------------|---------------------|---------------------|
| 1          | LLaMA-3-70B                | LLaMA-3-70B                | LLaMA-3-70B         | LLaMA-3-70B         | LLaMA-3-70B         | LLaMA-3-70B         | LLaMA-3-70B      | LLaMA-3-70B         | LLaMA-3-70B         |
| 2          | GPT-4o-mini                | GPT-4o-mini                | GPT-4o-mini         | GPT-4o-mini         | GPT-4o-mini         | GPT-4o-mini         | GPT-4o-mini      | GPT-4o-mini         | GPT-4o-mini         |
| 3          | o1-mini                    | o1-mini                    | o1-mini             | o1-mini             | o1-mini             | o1-mini             | o1-mini          | o1-mini             | o1-mini             |
| 4          | Gemini-1.5-Flash           | <b>LLaMA-3.1-8B</b>        | <b>LLaMA-3.1-8B</b> | Gemini-1.5-Flash    | <b>LLaMA-3.1-8B</b> | <b>LLaMA-3.1-8B</b> | Gemini-1.5-Flash | <b>LLaMA-3.1-8B</b> | <b>LLaMA-3.1-8B</b> |
| 5          | Mistral-7B                 | Gemini-1.5-Flash           | Gemini-1.5-Flash    | <b>LLaMA-3.1-8B</b> | Gemini-1.5-Flash    | <b>LLaMA-3.1-8B</b> | Gemini-1.5-Flash | Gemini-1.5-Flash    | Mistral-7B          |
| 6          | Claude-3-Haiku             | Mistral-7B                 | Mistral-7B          | Mistral-7B          | Mistral-7B          | Mistral-7B          | Mistral-7B       | Mistral-7B          | Claude-3-Haiku      |
| 7          | <b>LLaMA-3.1-8B</b>        | Claude-3-Haiku             | Claude-3-Haiku      | Claude-3-Haiku      | Claude-3-Haiku      | Claude-3-Haiku      | Claude-3-Haiku   | Claude-3-Haiku      | <b>LLaMA-3.1-8B</b> |
| 8          | LLaMA-3.2-3B               | LLaMA-3.2-3B               | LLaMA-3.2-3B        | LLaMA-3.2-3B        | LLaMA-3.2-3B        | LLaMA-3.2-3B        | LLaMA-3.2-3B     | LLaMA-3.2-3B        | LLaMA-3.2-3B        |
| <b>FDR</b> | —                          | —                          | 0.099               | 0.084               | 0.097               | 0.083               | 0.095            | 0.087               | <b>0.032</b>        |

1216

1217

1218 10%, 25% and 50% contamination (Tables 8, 9, 10 and 11 for SimpleQA benchmark). The model  
 1219 ranking on SimpleQA serves as the ground truth for evaluating model performance under clean  
 1220 conditions, as shown in the second column of Tables (SimpleQA (Ground Truth)). To simulate  
 1221 contamination, we randomly select 5%, 10%, 25% and 50% of the SimpleQA dataset to fine-tune  
 1222 LLaMA-3.1-8B, thereby introducing artificial contamination. We then evaluate this fine-tuned model  
 1223 on the full SimpleQA dataset, with results shown in the SimpleQA (contaminated) column of Table 2.  
 1224 Next, to assess the effectiveness of training data detection, we apply various detection methods to  
 1225 identify and retain only the clean data from the evaluation set. We then evaluate the relative rankings  
 1226 of the eight models based on their performance. The closer these rankings are to the ground truth,  
 1227 the more effective the detection method. For each setting, we report the FDR of different training  
 1228 data detection methods, defined as the proportion of contaminated samples incorrectly identified as  
 1229 clean among all samples predicted to be clean. From Tables 8, 9, 10 and 11, we have the following  
 1230 conclusions:

- *Finding 1 – Data contamination severely compromises fair model evaluation.* We find that data contamination significantly affects the fairness of model evaluation. Moreover, the degree of contamination is positively correlated with the extent of the impact: the higher the contamination level, the more the evaluation is skewed. For example, under 5% contamination, LLaMA-3.1-8B moves from rank 7 to rank 5; however, with 25% contamination, it rises further to rank 2.
- *Finding 2 – Existing training data detection methods are helpful but not yet sufficient.* All detection methods help mitigate contamination to some extent—as evidenced by the fact that the contaminated LLaMA-3.1-8B ranks lower than in the fully contaminated case. However, its rank remains higher than the ground-truth position (7th), indicating that residual contamination persists.
- *Finding 3 – TD4Eval effectively mitigates the impact of data contamination on model evaluation.* Across all contamination levels, TD4Eval consistently achieves the lowest FDR, demonstrating its strong ability to identify clean evaluation data. Notably, under TD4Eval, the ranking of LLaMA-

1242

1243 Table 10: Impact of different detection methods on LLM Evaluation. We simulate a data contami-  
 1244 nation scenario by fine-tuning LLaMA-3.1-8B on 25% of the SimpleQA training set. Various data  
 1245 detection methods are then employed to retain clean data for LLM evaluation. The effectiveness of a  
 1246 detection method is measured by how closely the resulting model leaderboard aligns with the ground  
 1247 truth ranking, the closer the match, the more effective the method.

| Rank       | SimpleQA<br>(Ground Truth) | SimpleQA<br>(contaminated) | PPL                 | Lowercase           | Zlib                | Grad                | Min-K%              | Min-K%++            | TD4Eval             |
|------------|----------------------------|----------------------------|---------------------|---------------------|---------------------|---------------------|---------------------|---------------------|---------------------|
| 1          | LLaMA-3-70B                | LLaMA-3-70B                | LLaMA-3-70B         | LLaMA-3-70B         | LLaMA-3-70B         | LLaMA-3-70B         | LLaMA-3-70B         | LLaMA-3-70B         | LLaMA-3-70B         |
| 2          | GPT-4o-mini                | <b>LLaMA-3.1-8B</b>        | GPT-4o-mini         |
| 3          | o1-mini                    | GPT-4o-mini                | o1-mini             |
| 4          | Gemini-1.5-Flash           | o1-mini                    | <b>LLaMA-3.1-8B</b> | <b>LLaMA-3.1-8B</b> | <b>LLaMA-3.1-8B</b> | <b>LLaMA-3.1-8B</b> | <b>LLaMA-3.1-8B</b> | <b>LLaMA-3.1-8B</b> | Gemini-1.5-Flash    |
| 5          | Mistral-7B                 | Gemini-1.5-Flash           | Gemini-1.5-Flash    | Gemini-1.5-Flash    | Gemini-1.5-Flash    | Gemini-1.5-Flash    | Gemini-1.5-Flash    | Gemini-1.5-Flash    | Mistral-7B          |
| 6          | Claude-3-Haiku             | Mistral-7B                 | Claude-3-Haiku      |
| 7          | <b>LLaMA-3.1-8B</b>        | Claude-3-Haiku             | Mistral-7B          | Mistral-7B          | Mistral-7B          | Mistral-7B          | Mistral-7B          | Mistral-7B          | <b>LLaMA-3.1-8B</b> |
| 8          | LLaMA-3.2-3B               | LLaMA-3.2-3B               | LLaMA-3.2-3B        | LLaMA-3.2-3B        | LLaMA-3.2-3B        | LLaMA-3.2-3B        | LLaMA-3.2-3B        | LLaMA-3.2-3B        | LLaMA-3.2-3B        |
| <b>FDR</b> | —                          | —                          | 0.162               | 0.152               | 0.166               | 0.114               | 0.171               | 0.133               | <b>0.046</b>        |

1255

1256

1257 Table 11: Impact of different detection methods on LLM Evaluation. We simulate a data contami-  
 1258 nation scenario by fine-tuning LLaMA-3.1-8B on 50% of the SimpleQA training set. Various data  
 1259 detection methods are then employed to retain clean data for LLM evaluation. The effectiveness of a  
 1260 detection method is measured by how closely the resulting model leaderboard aligns with the ground  
 1261 truth ranking, the closer the match, the more effective the method.

| Rank       | SimpleQA<br>(Ground Truth) | SimpleQA<br>(contaminated) | PPL                 | Lowercase           | Zlib                | Grad                | Min-K%              | Min-K%++            | TD4Eval             |
|------------|----------------------------|----------------------------|---------------------|---------------------|---------------------|---------------------|---------------------|---------------------|---------------------|
| 1          | LLaMA-3-70B                | LLaMA-3-70B                | LLaMA-3-70B         | LLaMA-3-70B         | LLaMA-3-70B         | LLaMA-3-70B         | LLaMA-3-70B         | LLaMA-3-70B         | LLaMA-3-70B         |
| 2          | GPT-4o-mini                | <b>LLaMA-3.1-8B</b>        | o1-mini             | GPT-4o-mini         | GPT-4o-mini         | GPT-4o-mini         | o1-mini             | GPT-4o-mini         | GPT-4o-mini         |
| 3          | o1-mini                    | GPT-4o-mini                | GPT-4o-mini         | o1-mini             | o1-mini             | o1-mini             | GPT-4o-mini         | o1-mini             | o1-mini             |
| 4          | Gemini-1.5-Flash           | o1-mini                    | <b>LLaMA-3.1-8B</b> | <b>LLaMA-3.1-8B</b> | <b>LLaMA-3.1-8B</b> | <b>LLaMA-3.1-8B</b> | <b>LLaMA-3.1-8B</b> | <b>LLaMA-3.1-8B</b> | Gemini-1.5-Flash    |
| 5          | Mistral-7B                 | Gemini-1.5-Flash           | Mistral-7B          | Mistral-7B          | <b>LLaMA-3.1-8B</b> | Mistral-7B          | Mistral-7B          | Gemini-1.5-Flash    | Mistral-7B          |
| 6          | Claude-3-Haiku             | Mistral-7B                 | Gemini-1.5-Flash    | Gemini-1.5-Flash    | Gemini-1.5-Flash    | Mistral-7B          | Gemini-1.5-Flash    | Mistral-7B          | Claude-3-Haiku      |
| 7          | <b>LLaMA-3.1-8B</b>        | Claude-3-Haiku             | Claude-3-Haiku      | Claude-3-Haiku      | Claude-3-Haiku      | Claude-3-Haiku      | Claude-3-Haiku      | Claude-3-Haiku      | <b>LLaMA-3.1-8B</b> |
| 8          | LLaMA-3.2-3B               | LLaMA-3.2-3B               | LLaMA-3.2-3B        | LLaMA-3.2-3B        | LLaMA-3.2-3B        | LLaMA-3.2-3B        | LLaMA-3.2-3B        | LLaMA-3.2-3B        | LLaMA-3.2-3B        |
| <b>FDR</b> | —                          | —                          | 0.223               | 0.248               | 0.234               | 0.108               | 0.199               | 0.172               | <b>0.025</b>        |

1270 3.1-8B exactly matches its ground-truth position, highlighting that controlling FDR is crucial for  
 1271 reducing the impact of data contamination on model evaluation.

1272

1273

### 13 APPENDIX E

1274

1275 In this section, we discuss the limitations of TD4Eval. While TD4Eval demonstrates strong perfor-  
 1276 mance in controlling the FDR and maximizing detection power, certain limitations remain. Specifi-  
 1277 cally, to balance FDR control with high detection power, we introduce a fusion strategy that integrates  
 1278 multiple detection techniques into the classical BH procedure. However, the effectiveness of this  
 1279 framework depends heavily on the quality of the underlying detection methods. If the base detectors  
 1280 (e.g., Min-K% Li (2023), Min-K%++ Li (2023)) fail to capture specific contamination patterns,  
 1281 the aggregated detection signal may remain weak, potentially resulting in undetected contaminated  
 1282 samples. In future work, we aim to develop more powerful detection methods to further mitigate the  
 1283 impact of test data contamination.

1284

### 14 THE USE OF LARGE LANGUAGE MODELS

1285

1286 According to the ICLR 2026 conference guidelines on the use of LLMs, we only employed LLMs to  
 1287 refine the text of this paper. We ensured that this refinement process did not alter the core ideas or  
 1288 compromise the academic rigor of the original content.

1289

1290

1291

1292

1293

1294

1295